ACCSCIENCE PUBLISHING

International Journal of Bioprinting

REVIEW ARTICLE

Advanced 3D bioprinting for bone oncology research

Miao Wang[1], Tingyao Zang[1], Xinghong Sun[1,2], Xiangran Cui[1,2]*, and Ning Wang[1,2]*

[1]Liaoning University of Traditional Chinese Medicine, Shenyang, Liaoning, China

[2]Department of Oncology, Second Affiliated Hospital of Liaoning University of Traditional Chinese Medicine, Shenyang, Liaoning, China

Abstract

Bone tumors are malignant diseases that pose a serious threat to human health, with an increasing incidence rate. Traditional two-dimensional cell cultures and mouse xenograft models have limitations in replicating the complexity of the tumor microenvironment and in accurately mimicking in vivo physiological conditions. Three-dimensional bioprinting technology, as an advanced biofabrication technique, can efficiently, economically, and consistently construct tumor models with complex geometric structures by precisely controlling the spatial distribution of cells, growth factors, and biomaterials. Three-dimensional printed bone tumor models based on bioinks possess higher biological fidelity and physiological relevance, realistically recreating the complex structure and function of the tumor microenvironment and accurately simulating tumor heterogeneity, cell migration, proliferation, invasion, and intercellular interactions. This technology can not only effectively simulate key biological processes of tumor development and progression but also accurately evaluate the response of tumor cells to novel anticancer drugs, supporting the realization of personalized precision medicine. Therefore, three-dimensional bioprinting technology provides a powerful scientific tool and new research ideas for the mechanistic study of bone tumors, the screening and optimization of anticancer drugs, and the development of personalized treatment plans.

Keywords: 3D bioprinting; Tumor microenvironment; Bone tumors; In vitro models; Precision medicine

***Corresponding authors:**
Xiangran Cui
(1334367621@qq.com)
Ning Wang
(xb210803@yeah.net)

Citation: Wang M, Zang T, Sun X, Cui X, Wang N. Advanced 3D bioprinting for bone oncology research. *Int J Bioprint.* 2026;12(3):026130115. doi: 10.36922/IJB026130115

Received: March 24, 2026

1st revised: April 18, 2026

2nd revised: May 6, 2026

Accepted: May 13, 2026

Published online: May 13, 2026

1. Introduction

Bone tumors are malignant diseases that seriously threaten human health. In recent years, their incidence has been rising, and primary malignant bone tumors are particularly common in adolescents and middle-aged adults, including osteosarcoma, Ewing sarcoma, and chondrosarcoma.[1,2] Bone tumors can cause severe pain and pathological fractures, and may even lead to nerve compression and impaired motor function, greatly affecting patients' quality of life.[3,4] In addition, bone is a common site of metastasis for malignant tumors; this not only indicates disease progression and poor prognosis but can also trigger pathological fractures and skeletal instability, leading to spinal cord compression and related events, further increasing patient suffering. Therefore, in-depth

study of the molecular biology of bone tumors, especially the interactions and metastatic mechanisms between bone tumors and other organ malignancies (such as breast cancer and prostate cancer), is of great significance for developing new diagnostic and therapeutic approaches and improving patient outcomes.[5-7] To deepen research in tumor pathology and facilitate the development of novel anti-tumor therapeutic strategies, researchers have constructed various in vitro and in vivo tumor model systems.[8,9]

While traditional two-dimensional (2D) cell culture can provide preliminary insights into tumor pathogenesis, its limitations lie in its inability to accurately replicate the complexity of the in vivo microenvironment. The biological behavior of tumor cells in vivo is regulated by multiple factors, including cell–cell communication, cell–extracellular matrix interactions, and chemotaxis, leading to significant discrepancies between results from 2D models and the in vivo situation.[10,11] In recent years, numerous studies have confirmed that three-dimensional (3D) systems have distinct advantages in terms of physiological relevance, as they can more realistically simulate the migration and proliferation of tumor cells in vivo. They also demonstrate higher accuracy in assessing tumor drug sensitivity, making 3D culture technology an important tool for constructing complex tumor models.[12,13] In contrast, although murine xenograft models have certain application value, they have shortcomings in replicating specific tumor microenvironments due to the tendency of the tumor matrix to be replaced by the host matrix.[14,15] Tumor models established in immunodeficient mice, in particular, cannot accurately represent the tumor immune microenvironment and also face multiple constraints, including ethical considerations, high economic costs, and differences in technical operations.[16,17] Therefore, the widespread application of in vitro model systems fully demonstrates their enormous potential in medical tissue engineering.

Supported by computer-aided design, 3D bioprinting technology, as an innovative development of traditional additive manufacturing, has opened new avenues for the development and in-depth exploration of novel diagnostic and therapeutic strategies for bone tumors.[18,19] Compared with conventional 3D printing, this technology employs multiple bioprinting methods, such as extrusion, inkjet, and photopolymerization, to precisely deposit material layer by layer. Centered on bioinks (active substances composed of biomaterials and biological units), it accurately controls the spatial distribution of cells, growth factors, and biomaterials to construct living structures.[20,21] Bioinks should possess printability, biocompatibility, appropriate mechanical properties, and biological stability, and their selection must be customized according to the specific structure of the tumor tissue and the intended biological behavior. This enables efficient, economical, consistent, and high-throughput creation of tumor models with complex geometries.[22-24]

Bone tumor models constructed by 3D bioprinting exhibit greater biomimicry and physiological relevance. These models can faithfully reproduce the complex structure and functions of the tumor microenvironment, simulating the heterogeneity of tumors, including cell arrangement, morphology, migration, invasion, and cell-cell and cell-matrix interactions.[25,26] Their advantages lie not only in effectively modeling key biological processes such as tumor cell migration, proliferation, and invasion, but also in more accurately assessing tumor cell responses to novel anticancer drugs.[27,28] At the same time, bioprinting enhances the long-term stability and manipulability of tumor models by layer-by-layer stacking of cells and scaffold materials, and supports customized construction—particularly reproducing individualized disease mechanisms and drug responses using patient-derived cells. Therefore, 3D bioprinting technology provides a solid scientific foundation for elucidating the mechanisms of bone tumor development and progression, systematically screening and optimizing anticancer drugs, and formulating personalized treatment plans. As an ideal method for constructing in vitro tumor organ models with batch-to-batch consistency and reproducibility, it offers powerful tools and new approaches for oncology research.[29-31]

This review systematically summarizes contemporary studies that employ advanced bioprinting technologies to construct bone tumor organoid models. Distinct from previous literature, this review provides a critical evaluation of how specific bioprinting modalities and bioink formulations influence the biomimicry of the bone tumor microenvironment. Table 1 offers a detailed compilation of existing models, while Tables 2 and 3 provide a rigorous comparison of printing techniques and material properties, offering a practical roadmap for researchers to select optimal platforms for their specific oncological studies. By bridging the gap between technological capabilities and biological requirements, this review clarifies the limitations of current models and provides forward-looking insights into the implementation of 4D bioprinting for bone oncology. Ultimately, this work serves as a comprehensive resource to stimulate innovation in drug screening and the development of personalized therapeutic strategies (Figure 1).

Table 1. Bioprinting preparation of in vitro bone tumor models

Tumor type	Method	Cell species	Cell type	Bioink	Summary	Reference
Osteosarcoma	3D bioprinting based on extrusion	Human	MG63	Alginate-GelMA	SBAW-assisted patterning achieves controllable anisotropic cellular patterns with high viability.	[32]
	3D bioprinting based on extrusion	Human	MG63	GG–SA/TMP-BG	Composite hydrogel bioink with good printability, biocompatibility, and osteochondral repair potential.	[33]
	3D bioprinting based on extrusion	Human	HOS, 143B, U2-OS	GelMA/HAMA	Multi-omics and drug screening platform mimicking the native tumor microenvironment.	[34]
	3D bioprinting based on extrusion	Human	U-2OS/ CDDP1	Collagen-based hydrogel	Physiologically relevant platform for studying invasion and chemosensitivity, including cisplatin resistance.	[35]
	3D bioprinting based on extrusion	Human	MG-63	PLA/MBG	Investigated mechanical stiffness effects on MG-63 behavior; confirmed support for osteogenic differentiation (ALP expression).	[36]
	3D bioprinting based on extrusion	Human, mouse	MG63, ST2, BMSCs	ADA-GEL/ Cu-MBGNs	HA-enriched scaffolds promoted spheroid formation; effectively used for evaluating cisplatin and doxorubicin efficacy.	[37]
	3D bioprinting based on extrusion	Rat	UMR-106	GE-CH/PEG-MA	Developed stable multi-layer scaffolds with high viability; established a reliable 3D model for osteosarcoma research.	[38]
	3D bioprinting based on extrusion	Human	MG-63	GelMA/8-PEGTA	High-viscosity bioink with enhanced mechanical strength (125–245 kPa); promoted both osteogenesis and angiogenesis.	[39]
	3D bioprinting based on extrusion	Human	143B-luc-RFP	GelMA	Created hollow microfibers to simulate cell invasion and tubule-like structure formation in the tumor microenvironment.	[40]
	3D bioprinting based on extrusion	Human, SD rats	SAOS-2	GelMA/MeCFO	Excellent pore structure and biocompatibility; suitable for both tumor modeling and bone tissue engineering applications.	[41]
	Pneumatic extrusion-based 3D bioprinter	Rat	UMR-106	Gelatin-sodium alginate	Optimized protocol for 3D-bioprinted osteosarcoma model for BNCT applications.	[42]
	3D bioprinting based on extrusion	Human	U-2 OS/ MG-63	1% sodium alginate/6% gelatin	Demonstrated CDK4/6 inhibitor efficacy in reducing sarcoma cell viability and stemness.	[43]
	3D bioprinting based on extrusion	Human	MG-63	ADA-GE/SPPs	A silica nanoparticle-enhanced bioink with improved printability and cell viability.	[44]
	3D bioprinting based on extrusion	Human, SD rats	MC3T3-E1, MG-63	ADA-GEL-FA	An antibacterial and antioxidant hydrogel supporting osteoblast proliferation while inhibiting tumor cells.	[45]

(*cont'd...*)

Table 1. (*Continued*)

Tumor type	Method	Cell species	Cell type	Bioink	Summary	Reference
	3D bioprinting based on extrusion	Human, SD rats	MG63, L929	BSA-alginate/PEC-GC	Nanofibrous polyelectrolyte complex bioink; >90% viability and osteogenic potential.	[46]
	3D bioprinting based on extrusion	Human	SaOS-2	QSH/GelQSH/P11-4 peptide	Peptide-functionalized bioink with enhanced mineralization for dental tissue engineering.	[47]
	3D bioprinting based on extrusion	Human	MG-63, HUVECs	GelMA-HA	Microfluidic osteosarcoma-on-a-chip; enhanced drug sensitivity in a dynamic environment.	[48]
	Embedded bioprinting technology	Human	MG-63	AlgMA/GelMA	Gradient biomechanical signal model advancing insights into tumor development and drug screening.	[49]
	3D bioprinting based on extrusion	Human	Saos-2	7.5% GelMA/0.2% nHA	Osteomimetic inks mimicking bone composition for disease mechanism and drug screening.	[50]
	3D bioprinting based on extrusion	Human	SaOS-2	Alginate-PRP	PRF-enriched bioinks significantly improve cell viability and scaffold integrity.	[51]
	3D bioprinting based on extrusion	Human	MG-63	GelMA-MC-ALG/dECM	Osteosarcoma spheroids in dECM-enriched bioink for simulating chemotherapy resistance.	[27]
Multiple myeloma	3D bioprinting based on extrusion	Human	OPM2, L363	O-MSC-CPC	Two-compartment bone marrow model for studying myeloma cell interactions and drug screening.	[52]
	Coaxial nozzle extrusion bioprinting	Human	MM1S, RPMI-8226	5% w/v GelMA, 0.25% w/v PI, nHA/PEGDA	Coaxial bioprinted model for investigating BTZ and TOC drug responses in myeloma.	[53]
Breast cancer	3D bioprinting based on light	Human	BrCa cell, MSCs	GelMA-nHA	Established in vitro model for studying breast cancer bone invasion and metastasis.	[54]
	3D bioprinting based on extrusion	Human	MDA-MB-231, HUVECs	GelMA/PEGDA/HAP	Developed a tumor–vessel–bone co-culture model for breast cancer bone metastasis and drug evaluation.	[22]
	3D bioprinting based on extrusion	Human	MDA-MB-231	1% alginate/7% gelatin	Developed tumor-stroma co-culture model for selective CAP therapy in bone metastases.	[55]
	3D bioprinting based on extrusion	Human	MDA-MB-231, MCF-7	ColMA-HAMA/GelMA-nHA	Microfluidic platform simulating bone metastasis; studies proliferation, migration, and invasion.	[56]
	3D bioprinting based on extrusion	Human	MDA-MB-231, MCF-7	μRB	Gelatin ribbon microgel bioink for anisotropic constructs; applied to a bone metastasis model.	[57]

(*cont'd...*)

Table 1. (*Continued*)

Tumor type	Method	Cell species	Cell type	Bioink	Summary	Reference
Carcinoma of the prostate	3D bioprinting based on extrusion	Human	C4-2B, PC-3	dECM-CPC	Biomimetic bone niche reconstructing enzalutamide-resistant prostate cancer bone metastasis.	[58]
Acute myeloid leukemia	Robotic multicellular bioprinting system	Human	KG1a, HL-60, MV4-11, Primary AML samples	Ac/-Lys-NH2	3D bone marrow niche AML model for studying drug resistance and disease relapse.	[59]
Tumor microenvironment	3D bioprinting based on extrusion	Human	MSCs, Tu167	DeepFreeze-3D	Cryogenic biofabrication for off-the-shelf large-scale tissue analogs with stem cell differentiation.	[29]

Abbreviations: 8-PEGTA: 8-arm polyethylene glycol tetraacrylate; ADA: Alginate dialdehyde; AGA-GE/SPP: Agarose–gelatin/sodium polyphosphate; AlgMA: Alginate methacrylate; ALP: Alkaline phosphatase; AML: Acute myeloid leukemia; BMSC: Bone marrow mesenchymal stem cell; BNCT: Boron neutron capture therapy; BSA: Bovine serum albumin; BTZ: Bortezomib; CAP: Cold atmospheric plasma; CDK: Cyclin-dependent kinase; ColMA: Collagen methacrylate; CPC: Calcium phosphate cement; Cu-MBGN: Copper-doped mesoporous bioactive glass nanoparticles; dECM: Decellularized extracellular matrix; GE-CH: Gelatin–chitosan; GEL: Gelatin; GEL-FA: Gelatin functionalized with folic acid; GelMA: Gelatin methacryloyl; GelMA-MC-ALG: Gelatin methacryloyl–methylcellulose–alginate; GG–SA: Gellan gum–sodium alginate; HA: Hyaluronic acid; HAMA: Hyaluronic acid methacrylate; HAP: Hydroxyapatite; HUVEC: Human umbilical vein endothelial cell; MBG: Mesoporous bioactive glass; MeCFO: Methacrylated fish collagen; MSC: Mesenchymal stem cell; nHA: Nanohydroxyapatite; O-MSC-CPC: Osteogenic mesenchymal stem cell–calcium phosphate cement; PEC-GC: Polyelectrolyte complex–glycol chitosan; PEG-MA: Polyethylene glycol methacrylate; PEGDA: Polyethylene glycol diacrylate; PI: Photoinitiator; PLA: Polylactic acid; PRF: Platelet-rich fibrin; PRP: Platelet-rich plasma; SBAW: Standing bulk acoustic wave; TMP-BG: Trimetaphosphate bioactive glass; TOC: Total organic carbon; μRB: Microribbon.

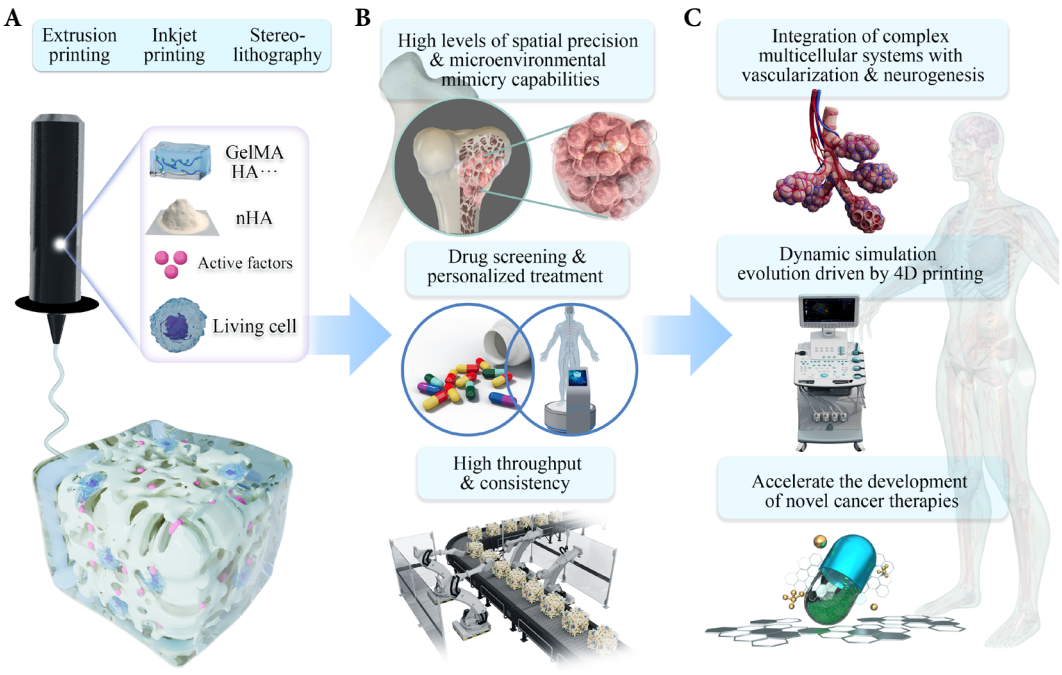

Figure 1. Schematic diagram of 3D-bioprinted bone tumor model. (A) In vitro bone tumor models are built using various 3D bioprinting technologies in conjunction with specific bioinks. (B) Significant advantages of the bone tumor models: They possess a high degree of biomimicry (high fidelity) and support high-throughput drug screening. (C) Future trend. In the future, 3D bioprinting will evolve into 4D bioprinting by introducing complex vascular systems to further simulate and restore the authentic tumor microenvironment.
Abbreviations: GelMA: Gelatin methacryloyl; HA: Hyaluronic acid.

Table 2. Comparison of 3D bioprinting techniques for bone tumor models

Method	Principle/Key features	Advantages	Limitations	Applications
Inkjet-based bioprinting	Thermal/piezoelectric actuation ejects low- to moderate-viscosity bioink droplets layer by layer.	Low cost, high speed, high viability, low shear stress; supports multi-material printing and microvasculature.	Sensitive to ink viscosity/surface tension; prone to nozzle clogging; difficult for high-viscosity or multi-component materials.	High-viability models for early metastasis; multi-material tumor composites; high-throughput drug screening.
Extrusion-based bioprinting	Continuous mechanical pressure extrudes bioink filaments; compatible with high-viscosity hydrogels and dECM.	Wide viscosity range, high cell density, strong mechanical integrity; advanced variants (coaxial, FRESH) enable tubular networks and gradients.	Shear stress at the nozzle reduces viability; resolution is limited by nozzle diameter, limiting micron-scale precision.	Large bone tumor models/resection scaffolds; vascularized tumor models; compositional gradient TMEs.
Stereolithography apparatus (SLA/DLP)	UV/visible light photocrosslinks low-viscosity bioinks layer by layer (or volumetrically).	High resolution (~10 μm); rapid speed; nozzle-free (no shear); precise mechanical control; complex internal channels.	Requires low-viscosity photocrosslinkable inks; UV may damage cells; two-photon polymerization is slow.	High-resolution bone architecture models; stiffness-controlled degradation models; constructs with intricate nutrient channels.
4D bioprinting	Smart, responsive materials enable printed constructs to evolve in response to external stimuli (e.g., temperature, light, pH).	Dynamic/adaptive tumor models; customizable microstructures; enables vascularization and cell–matrix interactions.	Material compatibility issues; limited long-term stability; complex design and fabrication.	Dynamic tumor models responsive to stimuli; studying stimuli-responsive drug delivery; adaptive post-resection regeneration scaffolds.
NEAT bioprinting	Microfluidic shear fields guide cell adhesion, differentiation, and matrix remodeling during printing.	Mimics native mechanical microenvironment; enhances tissue self-assembly and vascularization.	Non-uniform shear fields; biocompatibility under shear; scalability challenges for large constructs.	Models where cell alignment and mechanotransduction are critical (e.g., tumor invasion along the vasculature).
Scaffold-free spherical bioprinting	Self-assembly and volume-driven geometric adaptation without external scaffold support.	Stable intercellular networks and microvascularized channels; no scaffold boundary effects; enhances natural cell migration.	Biocompatibility constraints; assembly speed/scale control; stability optimization needed post-printing.	Tumor spheroids/organoids for high-throughput screening; early metastatic cluster models.
Microphysiological gradient-driven printing	Creates fine-grained physiological gradients (stiffness, nutrients, growth factors) within constructs.	Promotes differential differentiation; encourages vascularization; multi-scale structural/mechanical matching.	Precise gradient control required; biocompatibility in gradient systems; scalable production challenges.	High-fidelity TME models with oxygen/nutrient/pH gradients; tumor invasion across stiffness gradients.
Laser-induced forward transfer (LIFT)	Laser-induced deposition of minute material droplets for high-resolution multi-material assembly.	Ultra-high resolution; multi-material/level assembly; minimal cell damage; enables microvascular networks.	Strict thermal control needed; material compatibility limitations; large-scale coordination challenging.	Customized tumor models with intricate cellular patterns; localized multi-cell-type/drug placement; precision reconstruction post-resection.

Abbreviations: dECM: Decellularized extracellular matrix; DLP: Digital light processing; NEAT: Non-equilibrium assembling and trapping; TME: Tumor microenvironment.

Table 3. Comparison of bioinks for 3D bioprinting of bone tumor models

Bioink type	Source/Composition	Key properties	Advantages	Limitations	Applications
Alginate	Brown algae; natural linear polysaccharide; ionically crosslinked (Ca^{2+}).	High biocompatibility, low toxicity; porous structure; tunable viscosity.	Fast gelation, low cost, easy modification; mimics tumor ECM porosity.	Low mechanical strength; poor cell adhesion without RGD modification; slow degradation.	TME models; drug screening platforms; cell encapsulation.
Collagen	Most abundant mammalian ECM protein (Type I); thermo-sensitive gelation.	High cell affinity; mimics native bone ECM; good biodegradability.	Excellent native-like microenvironment; promotes osteogenesis and cell migration; good printability.	Low thermal stability (denatures >37 °C); poor mechanical strength; slow gelation, needs crosslinking.	High-fidelity in vitro tumor models; bone repair scaffolds post-resection; invasion/migration assays.
Chitosan	Deacetylated chitin (crustacean shells); cationic polysaccharide.	Intrinsic antibacterial; excellent osteoinductivity; good cell adhesion.	Biodegradable, antimicrobial; promotes bone regeneration; abundant and low-cost.	Low mechanical strength; pH-dependent solubility; limited print fidelity alone.	Tumor resection scaffolds; targeted drug delivery systems (pH-responsive); bone regeneration matrices.
Hyaluronic acid (HA)	Non-sulfated GAG; ubiquitous in ECM and TME; enzymatic degradation.	High hydration capacity; CD44 receptor-mediated signaling; excellent biocompatibility.	Actively participates in tumor cell signaling; high water retention; easily chemically modified.	Poor mechanical properties alone; rapid degradation; requires crosslinking for printability.	Tumor cell–ECM interaction studies; drug response in TME-like hydrogels; invasion and metastasis assays.
Silk fibroin (SF)	Fibroin protein from silkworm cocoons; β-sheet structure.	Exceptional mechanical toughness; slow degradation; biocompatible; supports osteogenesis.	High mechanical strength; versatile processing; can serve as a drug carrier; supports long-term culture.	Requires complex extraction/purification; limited cell adhesion without modification; slower degradation.	Bone tumor modeling (mechanical mimicry); post-resection bone defect scaffolds; sustained drug/protein delivery.

Abbreviations: ECM: Extracellular matrix; GAG: Glycosaminoglycan; TME: Tumor microenvironment.

2. Bioprinting materials and strategies

2.1. Bioprinting techniques

2.1.1. 3D bioprinting based on inkjet

Inkjet-based 3D bioprinting mimics the working principle of ordinary inkjet printers, precisely ejecting ink solutions containing living cells and biomaterials in the form of droplets that accumulate layer by layer to form 3D tissue structures.[60,61] Nozzle driving is typically achieved through mechanisms such as thermal, piezoelectric, and mechanical micro-cavity actuation, with thermal and piezoelectric methods being the most common: thermal actuation generates microdroplets through transient localized heating, while piezoelectric actuation achieves ejection by altering the pressure inside the nozzle using electrical signals.[62,63] The bioinks used are often hydrogel systems with controllable viscosity, commonly including gelatin, hydroxyethyl cellulose, gelatin-hyaluronic acid (HA) copolymers, and can encapsulate functional components such as living cells, growth factors, or nanoparticles within the droplets. An ideal bioink should possess low to moderate viscosity, good shear stability, rapid solidification or crosslinking, and good biocompatibility. The advantages of this technology include relatively low cost, relatively high printing speed, low shear stress exposure for microscopic cells, and the ability to perform material deposition in low-temperature environments, thereby improving cell viability and functional maintenance.[64,65] However, it also has limitations, such as sensitivity to ink viscosity, surface

tension, and nozzle clogging; difficulty in achieving stable ejection of high-viscosity or multi-component materials; and challenges in controlling density and mechanical properties during the layer-by-layer construction of highly complex geometric structures[66] (Figure 2A).

With a deeper understanding of the chemical and mechanical properties of bioinks, several specialized variations of inkjet-based bioprinting have emerged. One important direction is multi-material inkjet printing, which utilizes parallel or staggered printheads to assemble materials with different physical properties and cell types within the same layer, thereby constructing composite tissues with differentiated regions.[67,68] Another trend is the combination of self-assembly and embedded inkjet printing, where a hydrogel scaffold is initially printed to provide structural support, followed by subsequent jetting to build microvasculature, channels, or gland-like structures within the scaffold, aiming to enhance connectivity between internal cavities and conductive networks. Furthermore, the introduction of nanoparticles and functional molecules is expanding the performance of bioinks, for example, by using nanofibrillar cellulose or hydroxyapatite to enhance the mechanical strength of scaffolds or to guide cell behavior.[69,70] These variations aim to overcome the limitations of original inkjet printing in terms of material diversity, mechanical matching, and internal microstructure construction, thereby promoting the application potential of inkjet bioprinting in tissue regeneration, organ models, and drug screening platforms.[71]

2.1.2. 3D bioprinting based on extrusion

Extrusion-based 3D bioprinting is currently one of the most widely used techniques in the biomedical field. Its working principle is to generate continuous mechanical pressure via air pressure, a piston, or screw drive to extrude bioink from a fine nozzle in the form of filaments, and to deposit it layer by layer on a substrate along computer-prescribed paths to ultimately build a 3D solid structure.[72,73] This technique has strong compatibility with bioinks and can handle materials across a wide viscosity range; it is particularly suitable for high-viscosity hydrogels and decellularized extracellular matrix (dECM), and can even directly print thermoplastic polymer scaffolds. Its core advantages include the ability to achieve very high cell densities and to produce tissue constructs with good mechanical stability and structural integrity, making it well suited for manufacturing medium- to large-scale organ scaffolds.[74,75] However, its limitations are also notable: because it relies on physical extrusion, shear stress at the nozzle can damage cell membranes and affect cell viability, and its printing resolution is typically constrained by nozzle diameter, making it difficult to reach micron-scale precision.[76,77] Overall, extrusion printing shows strong application potential in tissue engineering, soft tissue models, and organ scaffold fabrication.[67]

As tissue-engineering demands have become more complex, extrusion-based bioprinting has evolved into a variety of highly specialized techniques. The most representative is coaxial extrusion printing, which uses specially designed multilayer nested nozzles to simultaneously extrude two or more different materials and build core–shell structured biofibers in one step; this is often used to mimic naturally occurring tubular or multilayer composite structures such as blood vessels, nerves, or muscles[78-80] (Figure 2B). Another breakthrough is embedded bioprinting (e.g., the FRESH technique), in which bioinks are extruded directly into a support bath with shear-thinning properties. The support bath provides buoyant support for uncrosslinked soft materials, effectively preventing collapse under gravity during printing and enabling the fabrication of complex overhanging structures such as heart valves or microvascular networks.[81,82] In addition, extrusion systems integrated with microfluidic chips enable real-time mixing and switching of components at the nozzle, making it possible to construct in vitro tissue models with complex compositional gradients and heterogeneity, greatly expanding the application boundaries of extrusion printing.

2.1.3. 3D bioprinting based on stereolithography

Lithography-based bioprinting is a technology that leverages photochemical reactions to precisely fabricate biomaterials. Its working principle involves irradiating photosensitive bioinks with ultraviolet or visible light, exciting photoinitiators to generate free radicals, and triggering photocrosslinking reactions, thereby solidifying the liquid bioink layer by layer into a 3D structure.[83,84] This method is suitable for bioinks containing photocrosslinkable functional groups, including naturally derived gelatin methacryloyl (GelMA), hyaluronic acid methacrylate (HAMA), dECM, and synthetic polyethylene glycol diacrylate and polyvinyl alcohol methacrylate.[85] The main limitations of stereolithography include: photocuring bioinks require low viscosity to remain liquid; some bioinks exhibit oxygen-inhibition problems, leading to uneven polymerization; ultraviolet light during manufacturing may cause cell damage; and layer-by-layer manufacturing limits the creation of true 3D volumetric structures. Its unique advantages lie in high resolution (down to 10 μm or less), rapid printing speed (especially with digital light processing technology), nozzle-free design avoiding shear stress damage to cells, precise control over mechanical properties and bioactivity, and the ability to construct bioscaffolds with complex internal channels and intricate

geometric features[86,87] (Figure 2C).

Based on the principles of photolithography, various specialized bioprinting methods have been developed. Volumetric bioprinting is the most groundbreaking derivative technology, overcoming the limitations of traditional layer-by-layer printing. It projects a series of 2D light patterns within the volume of bioink, which accumulate to form a 3D light dose distribution, simultaneously solidifying the entire construct in seconds and eliminating the need for layer-by-layer construction. This technique utilizes the principle of computed tomography with back-projection, making printing time independent of the construct volume and enabling the fabrication of centimeter-scale constructs in tens of seconds.[88,89] Two-photon polymerization, on the other hand, utilizes the nonlinear optical effect of infrared femtosecond lasers to simultaneously excite photosensitive molecules via two photons, achieving ultra-high-resolution fabrication at the deep sub-micron level. This allows the creation of complex microstructures, but the manufacturing speed is relatively slow.[90,91] Furthermore, multi-material stereolithography bioprinting achieves spatial distribution of multiple materials and cell types in a single process by sequentially changing or synchronously projecting different photosensitive bioinks, better mimicking the heterogeneity of biological tissues. These derivative technologies further expand the application scope of photolithography-based bioprinting, particularly holding significant promise for manufacturing larger-scale, more functionally complex tissue-engineering scaffolds.[92,93]

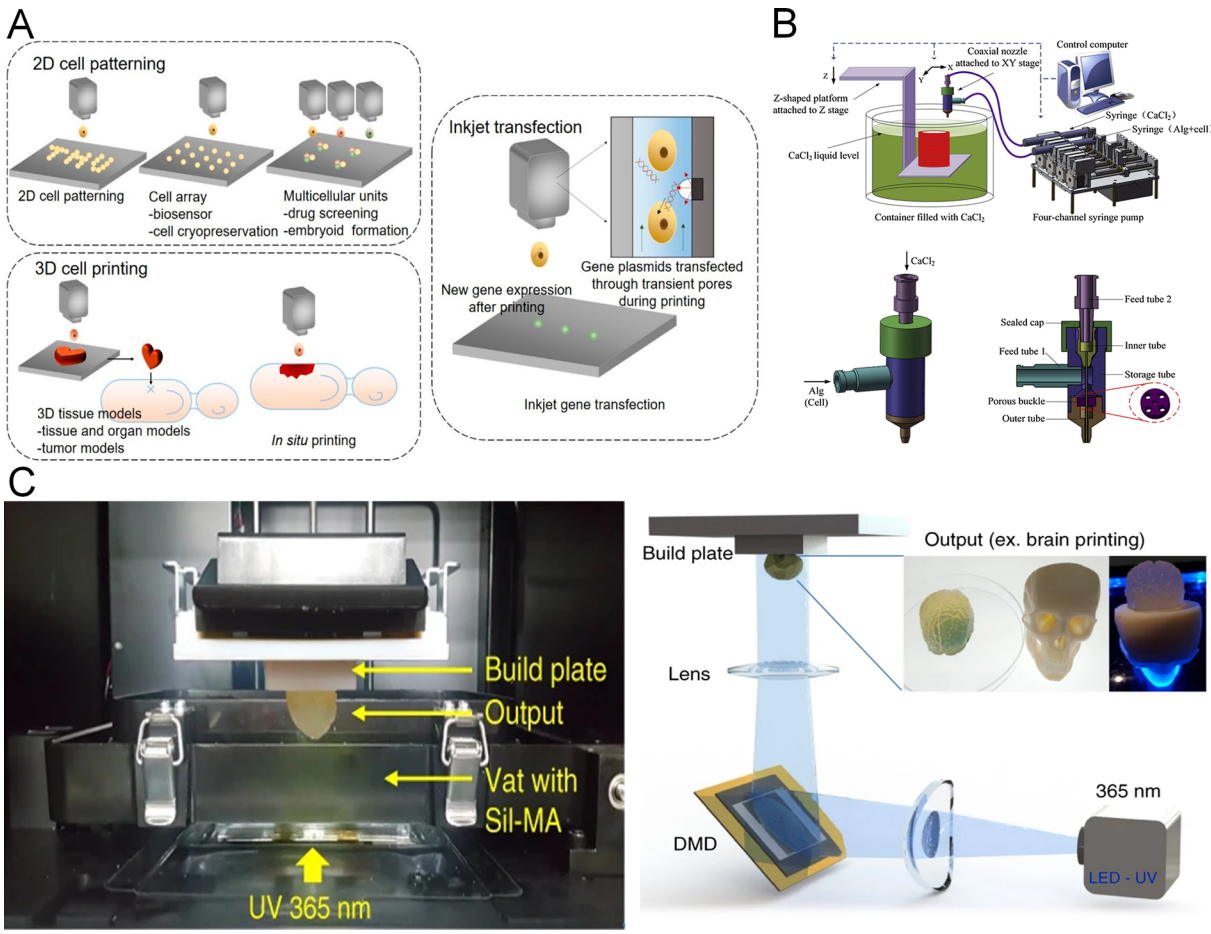

Figure 2. 3D bioprinting methods. (A) Strategies for bioprinting 3D cellular structures and some characteristic applications of inkjet cell printing. Reprinted with permission from Li *et al.*[94] Copyright 2020 AMER CHEMICAL SOC. (B) Coaxial nozzle-assisted 3D bioprinting system. Reprinted with permission from Gao *et al.*[95] Copyright 2015 ELSEVIER SCI LTD. (C) LAP-containing Sil-MA was printed layer-by-layer using a DLP printer. Reprinted with permission from Kim *et al.*[96]

Abbreviations: DLP: Digital light processing; DMD: Digital micromirror device; LAP: Lithium phenyl-2,4,6-trimethylbenzoylphosphinate; Sil-MA: Silicate methacrylate.

2.2. Other bioprinting technologies

2.2.1. 4D Bioprinting

Four-dimensional bioprinting extends conventional 3D bioprinting by incorporating a temporal dimension: after initial printing, the construct undergoes programmed, stimulus-triggered remodeling of its material properties, structure, or biochemical function. In bone tumor modeling, this capability is particularly important because the tumor microenvironment is inherently dynamic, evolving through changes in matrix stiffness, enzymatic activity, pH, oxygen gradients, and drug penetration profiles. Thus, 4D systems can bridge a critical gap between static 3D models and the temporal complexity of actual tumor progression and therapeutic response.[97]

Photo-responsive and thermo-responsive bioinks represent the most mature 4D strategies currently being integrated into bone tumor platforms. For example, photoresponsive hydrogels—such as those based on azobenzene-modified polymers, coumarins, or near-infrared chromophores—can undergo light-triggered crosslinking density changes, enabling researchers to selectively harden or soften regions of a printed osteosarcoma model post-fabrication. This is operationally relevant: after printing a soft, cell-friendly construct, spatial UV or visible-light exposure can increase local stiffness in specific zones to simulate the desmoplastic (fibrotic) regions adjacent to tumor cores, which are known to exhibit higher mechanical resistance and altered drug penetration. Temperature-responsive bioinks (poly(N-isopropylacrylamide)–based or chitosan–gelatin blends exhibiting reversible sol–gel transitions) have been demonstrated in bone tissue engineering workflows; such materials can be printed at elevated temperature (where they remain liquid), then cooled to physiological temperature to trigger gelation, and subsequently re-heated in situ to induce controlled softening or pore enlargement-a capability useful for mimicking temporal remodeling of the extracellular matrix during tumor progression.[98]

Meanwhile, pH-responsive drug release is a near-term, clinically motivated application for bone tumors. Recent evidence shows that osteosarcomas and Ewing tumors generate mildly acidic microenvironments (pH: 6.5–7.0) due to lactate secretion and hypoxic metabolic reprogramming. 4D bioinks incorporating pH-sensitive linkers (e.g., hydrazone or acetal bonds) or acid-labile crosslinks can be engineered to progressively degrade or release encapsulated chemotherapeutic agents (such as methotrexate or doxorubicin) as they encounter acidic zones, thereby enhancing local drug concentration while reducing systemic toxicity. When integrated into extrusion- or lithography-based bioprinting, such constructs enable temporally controlled drug-dose escalation that mimics in vivo pharmacokinetics more closely than static models-a critical capability for evaluating both drug efficacy and resistance emergence over multi-week culture periods.[99,100]

Despite its promise, the practical implementation of 4D bioprinting in bone oncology is constrained by several critical bottlenecks. These include the potential cytotoxicity of responsive materials during repeated stimulation, the challenge of synchronizing artificial response kinetics with biological timescales, and the inherent lack of reproducibility across complex material formulations. Furthermore, technical limitations in real-time 3D monitoring of internal remodeling and the difficulty of scaling stimulus gradients (e.g., light or pH) to centimeter-scale bone constructs remain significant hurdles that currently limit the transition of these platforms from proof-of-concept models to standardized, high-fidelity research tools.

2.2.2. Next-generation bioprinting technologies

To move beyond simplified static models, several emerging bioprinting modalities are being adopted to capture the multi-scale complexity of the bone tumor microenvironment. Precision-driven techniques, such as microphysiological gradient-driven printing and laser-induced forward transfer (LIFT), offer unparalleled capabilities in recreating the spatial and biochemical gradients inherent to bone malignancies. Bone tumors, particularly osteosarcoma and metastatic lesions, thrive in environments characterized by sharp gradients in oxygen tension (hypoxia), mineral density, and growth factor concentrations (e.g., transforming growth factor-beta [TGF-β] and vascular endothelial growth factor [VEGF]). Gradient-driven printing allows for the programmed deposition of bioinks with varying stiffness and nutrient profiles, effectively mimicking the transition from the rigid, mineralized bone matrix to the softer, highly proliferative tumor core.[101-103] Complementing this, LIFT bioprinting provides single-cell-level resolution, enabling the point-to-point placement of tumor cells, stromal cells (such as mesenchymal stem cells [MSCs] and osteoblasts), and vascular components at the tumor–bone interface. This high-precision arrangement is critical for studying the vicious cycle of bone destruction, in which the spatial proximity of heterogeneous cell types dictates the rate of bone resorption and tumor expansion.[104-106]

Furthermore, mechanobiological and scaffold-free assembly approaches, including non-equilibrium assembling and trapping (NEAT; shear-stress-driven) bioprinting and scaffold-free spherical assembly, address the dynamic and high-density nature of bone

tumor masses. The pathophysiology of bone tumors is heavily influenced by interstitial fluid pressure and fluid shear stress, which modulate tumor cell migration and epithelial–mesenchymal transition (EMT) through mechanotransduction pathways. NEAT bioprinting leverages controllable shear forces during the printing process not just as a fabrication parameter, but as a biological trigger to align matrix fibers and pre-stress cells, thereby better simulating the pressurized microenvironment of an intraosseous tumor.[107,108] In parallel, scaffold-free spherical bioprinting addresses the limitations of synthetic or natural hydrogel matrices, which can sometimes introduce confounding boundary effects or dilute cell-cell signaling. By utilizing cell spheroids as building blocks, this approach achieves the high cell density characteristic of solid tumor aggregates. These scaffold-free constructs promote robust endogenous extracellular matrix production and spontaneous microvascularization, providing a superior platform for evaluating drug penetration kinetics and the resistance mechanisms of dense tumor nests that are often shielded from systemic therapy.[109-111]

2.3 bioinks

2.3.1. Alginate-based bioinks

Alginate bioinks hold a significant position in 3D bioprinting due to their unique physicochemical properties and biocompatibility. Their core features include excellent biocompatibility, non-toxicity, and mild crosslinking conditions.[112] As a natural polymer extracted from brown algae, alginate is inexpensive and highly water-soluble. In the presence of divalent cations, it can rapidly form hydrogels through ionic crosslinking, a process that is gentle and harmless to cells, greatly ensuring cell viability. Alginate is often used as a base component in composite bioinks, in combination with other materials (such as gelatin, collagen, and hydroxyapatite) to compensate for its shortcomings while retaining its core advantages as a cell carrier. Its suitable conditions primarily include scenarios sensitive to cytotoxicity, systems requiring rapid and gentle gelation, and as a matrix material for multi-material bioprinting.[113,114]

In 3D bioprinting of bone tumors, alginate-based bioinks exhibit a range of distinctive advantages. First, their excellent biocompatibility and low immunogenicity provide an ideal microenvironment for tumor cells, host cells, and other bioactive components, ensuring high cell viability and functionality within printed constructs. Second, the mild ionic crosslinking process avoids factors that could damage tumor cells or embedded therapeutics, such as high temperatures, strong acids or bases, or UV irradiation, making alginate suitable for building viable tumor models and drug screening platforms.[30,55] Additionally, the porous structure and tunable degradation rate of alginate hydrogels mimic the complex microenvironment of bone tumors, promoting the diffusion of nutrients and oxygen and allowing cell proliferation, migration, and the secretion of metabolic products. By combining alginate inks with bone materials such as nanohydroxyapatite (nHA) or tricalcium phosphate, mechanical performance and osteoinductive properties can be effectively enhanced, offering great potential for developing in vitro models that more closely reflect true bone tumor pathology or for composite scaffolds used to repair bone defects after tumor resection.[115,116]

2.3.2. Collagen-based bioinks

Collagen, as the most abundant protein in mammals, is the gold standard material for constructing biomimetic bioinks. Its core features are outstanding bioactivity, very high cell affinity, and natural sequence recognition sites (such as the RGD sequence), which can directly induce cell adhesion, migration, and phenotype maintenance, perfectly mimicking the biochemical environment of the native extracellular matrix.[117,118] Collagen typically exists as an acidic solution in vitro. Upon entering near-neutral culture conditions, it readily forms a loosely arranged fiber network, resulting in insufficient mechanical strength and thermal/structural stability, making it difficult to support and maintain complex 3D overhanging or long-term culture structures required for bone tumor models. Accordingly, collagen-based bioinks primarily achieve printability and structural stability through process-level temperature control, gelation timing management (to avoid premature gelation), and shape fidelity enhancement. Examples include increasing concentration, adjusting pH, chemical modification (e.g., methacrylation to support crosslinking and curing), or composite with synthetic polymers (e.g., polycaprolactone) and bioceramics to balance printing efficiency with the mechanical/interfacial characteristics required for subsequent modeling.[119,120]

In 3D bioprinting for bone tumors, collagen-based bioinks offer unparalleled advantages in pathological simulation and functional repair. First, they can highly recapitulate the histological microenvironment of bone tumor development; through their characteristic triple-helix structure to bind to integrin receptors on tumor cell surfaces, they activate relevant signaling pathways, thereby faithfully reflecting tumor cell invasive growth, angiogenesis, and biological responses to chemotherapeutic drugs, making them an ideal matrix for constructing high-fidelity in vitro tumor models.[22,23] Second, in repairing bone defects after tumor resection, collagen demonstrates excellent osteoinductive potential:

it can recruit endogenous host mesenchymal stem cells and promote their differentiation toward the osteogenic lineage, accelerating the deposition and integration of new bone. By precisely controlling the orientation of collagen fibers and the crosslinking density, such bioinks not only provide necessary physical support but also serve as sustained-release carriers for bioactive factors, achieving the dual clinical goals of inhibiting tumor recurrence and promoting functional bone reconstruction.[35,121]

2.3.3. Chitosan-based bioinks

Chitosan-based bioinks, derived from the shells of crustaceans and constituting a natural cationic polysaccharide, exhibit intrinsic antibacterial activity and structural similarity to native amino glycosaminoglycans. Chitosan exhibits good film-forming and chelating abilities and, through its positively charged amino groups, can interact with negatively charged cell surfaces to effectively promote cell adhesion and sustain metabolic activity.[122,123] Researchers often employ chemical modification (e.g., carboxymethylation or the introduction of photo-crosslinkable groups) or composite formulations with other polymers (e.g., alginate or gelatin), using ionic interactions to achieve rapid solidification.[124,125] Its main applications include settings that require an antimicrobial microenvironment, pH-responsive controlled drug-release systems, and as a bioactive scaffold material for bone tissue engineering frameworks.[126]

In 3D bioprinting for bone tumors, chitosan-based bioinks demonstrate unique biological and clinical application potential. Their excellent osteoinductive properties effectively promote the osteogenic differentiation of BMSCs and accelerate mineral deposition, which is critical for repairing bone defects after tumor resection. Additionally, the amino groups of chitosan confer unique pH-responsive release characteristics, enabling targeted release of loaded antitumor drugs or bioactive factors in the mildly acidic pathological microenvironment of bone tumors, achieving integrated therapy and repair.[121,127] Furthermore, chitosan has excellent affinity for bioceramics such as hydroxyapatite, and composite printing can significantly enhance scaffold mechanical properties and closely mimic the physicochemical structure of native bone tissue. This biomimetic composite system not only provides an ideal platform for studying the dynamic interactions between tumor cells and bone matrix, but also offers an advanced material solution for precise reconstruction of bone tumors that combines antibacterial protection with functional repair.[115]

2.3.4. Hyaluronic acid-based bioinks

Hyaluronic acid-based bioinks have garnered significant attention in 3D bioprinting, particularly in simulating bone tumor microenvironments, due to their unique biological functions. Their core characteristics include excellent viscoelastic properties, high hydration capacity, and bioactivity as a key component of the native extracellular matrix.[128,129] As a non-sulfated glycosaminoglycan, HA plays a pivotal role in regulating cell adhesion, migration, and signaling. However, native HA exists as a linear, high-molecular-weight fluid under physiological conditions, lacking sufficient mechanical strength and self-supporting ability, resulting in poor direct printability. Consequently, researchers often employ chemical modification (e.g., methacrylation to form HAMA) or utilize dynamic covalent bonds (e.g., Schiff base reactions) to impart photocrosslinking or self-healing properties.[130,131] Its application is primarily suited for scenarios requiring the simulation of high-water-content tissue environments, demanding extremely high biocompatibility, and serving as a functional regulator in composite inks to improve shear-thinning characteristics during extrusion.

In 3D bioprinting for bone tumors, the advantages of HA-based bioinks are mainly reflected in their high fidelity in mimicking the pathological microenvironment and their precise regulation of tumor behavior. Studies have shown that CD44 receptors on the surface of bone tumor cells (such as osteosarcoma) bind specifically to HA; this interaction not only mediates tumor invasion and metastasis but also significantly affects cancer cell resistance to chemotherapeutic drugs.[56,132] Therefore, 3D-printed models constructed with HA can reproduce the biochemical context of tumor development more realistically than traditional synthetic materials, providing a high-fidelity platform for antitumor drug screening. In addition, HA has the potential to promote angiogenesis and osteogenic differentiation of mesenchymal stem cells in bone regeneration.[133,134] By compositing HA-based inks with hydroxyapatite or bioactive glass, HA bioinks can fabricate integrated scaffolds that both mimic the antitumor microenvironment and repair bone defects, showing great translational potential for precise functional reconstruction after tumor resection.

2.3.5. Silk fibroin-based bioink

Silk fibroin-based bioinks exhibit remarkable mechanical toughness, excellent biocompatibility, and controllable degradation rates in 3D bioprinting due to their unique molecular structure. A key characteristic of silk fibroin is its abundance of hydrophobic amino acids within its molecular chains, which, by inducing a β-sheet structural transition, allows for a phase change from a liquid to a stable hydrogel without the addition of chemical crosslinkers. This confers high structural integrity and mechanical strength to the

printed constructs.[135,136] Compared to alginate or collagen, silk fibroin offers superior processing flexibility and resistance to enzymatic degradation. However, silk fibroin gelation is typically slow, and its pure solution viscosity is relatively low. Consequently, its suitability for printing often requires optimization through shear induction, sonication, or compounding with high-viscosity polymers (such as gelatin or polyethylene glycol).[137-139] This type of ink is particularly well-suited for tissue engineering applications that require long-term structural support, high load-bearing capacity, and extremely low immunogenicity.

In 3D bioprinting for bone tumors, the advantages of silk fibroin-based bioinks mainly include dual support for accurately mimicking complex pathomechanical environments and for promoting bone regeneration. First, the very high mechanical strength and toughness of silk fibroin allow it to effectively mimic the physical properties of bone tissue, providing a 3D microenvironment with realistic mechanical cues for tumor cell growth, migration, and drug response, which are crucial for studying tumor invasion mechanisms in rigid matrices.[18,140] Second, silk fibroin has excellent mineralization-inducing capability, promoting deposition of calcium phosphate and markedly enhancing the osteogenic differentiation potential of mesenchymal stem cells, which is highly advantageous for filling bone defects after tumor resection. In addition, as an excellent drug carrier, silk fibroin can achieve sustained release of antitumor drugs by tuning its crystallinity, thereby inhibiting tumor recurrence while promoting new bone ingrowth. Its low inflammatory response and capacity for personalized shaping provide a solid material basis for developing engineered bone tumor models that integrate diagnosis, therapy, and repair.[141,142]

3. Bone tumor model for bioprinting

3.1. Primary bone and marrow tumors

3.1.1. Osteosarcoma

Firstly, in the foundational research and development of bioinks and manufacturing technologies, the research focus is on balancing printability with bioactivity and on introducing physical fields to enhance tissue anisotropy. Traditional hydrogels such as GelMA and alginate have successfully mimicked the mineralized components of bone tissue and improved mechanical strength by incorporating inorganic components like nHA or mesoporous bioactive glass;[36,50] Furthermore, to address cell damage caused by extrusion printing, researchers have significantly improved the survival rate of cells such as MG-63 by adding platelet-rich fibrin or utilizing shear-thinning properties[33,51] (Figure 3C). More groundbreaking, standing bulk acoustic wave technology has been introduced into the bioprinting process, achieving directional alignment of cells within viscous inks and reconstructing the anisotropic structure of bone tissue from a physical perspective[32] (Figure 3A). In addition, nanocomposite inks with dynamic covalent chemistry,[37] self-assembling peptide-enhanced hybrid materials,[47] and interpenetrating network structures formed by enzymatic secondary cross-linking[39] have collectively addressed the contradiction between scaffold stability and cell adhesion during long-term culture, laying the material foundation for durable and highly biomimetic bone tumor models.

Second, regarding the biological remodeling of the tumor microenvironment, research has shifted from simple cell seeding to deep integration of extracellular matrix biochemical signals and physical-mechanical features. Studies have confirmed that 3D-printed models better recapitulate the transcriptome and methylation profiles of osteosarcoma (OS) cells than 2D cultures[34] (Figure 3D and 3E), and introducing tumor cell-derived dECM can further induce P-glycoprotein overexpression, modeling in vivo drug-resistant phenotypes.[27] On the physical side, models with varying stiffness gradients prepared by adjusting GelMA density revealed that softer matrices more readily promote OS cell migration and tumorigenicity,[40] while an integrated gradient biomechanical signal model (IGBSTOM) successfully reproduced tumor nest structures and stem-like features[49] (Figure 3F). To further mimic dynamic microenvironments, microfluidic chip technology combined with 3D printing uses continuous fluid shear to induce higher invasiveness in OS cells[48] (Figure 3B). These multidimensional biomimetic strategies make in vitro models functionally closer to real pathological tissues.

Finally, in clinical diagnosis/treatment and the development and application of cutting-edge therapies, 3D bioprinting platforms have demonstrated predictive value and therapeutic potential that surpass those of traditional animal models. This technology has been widely used to evaluate the efficacy of CDK4/6 inhibitors (such as lerociclib) against pediatric sarcomas[43] and to assess the sustained-release effects and toxicity of chemotherapeutics, such as cisplatin, within collagen scaffolds.[35] For refractory osteosarcoma, researchers have developed printed scaffolds loaded with magnetic cobalt ferrite nanoparticles to achieve the dual functions of hyperthermia therapy and bone repair,[41] and have used 3D models as experimental platforms for boron neutron capture therapy, filling the translational gap between 2D experiments and animal studies.[42] In addition, by incorporating antitumor agents such as ferulic acid[45] or silver-coated silica nanoparticles[44] into the bioink, 3D-printed scaffolds not only serve as carriers for tumor research but are themselves evolving

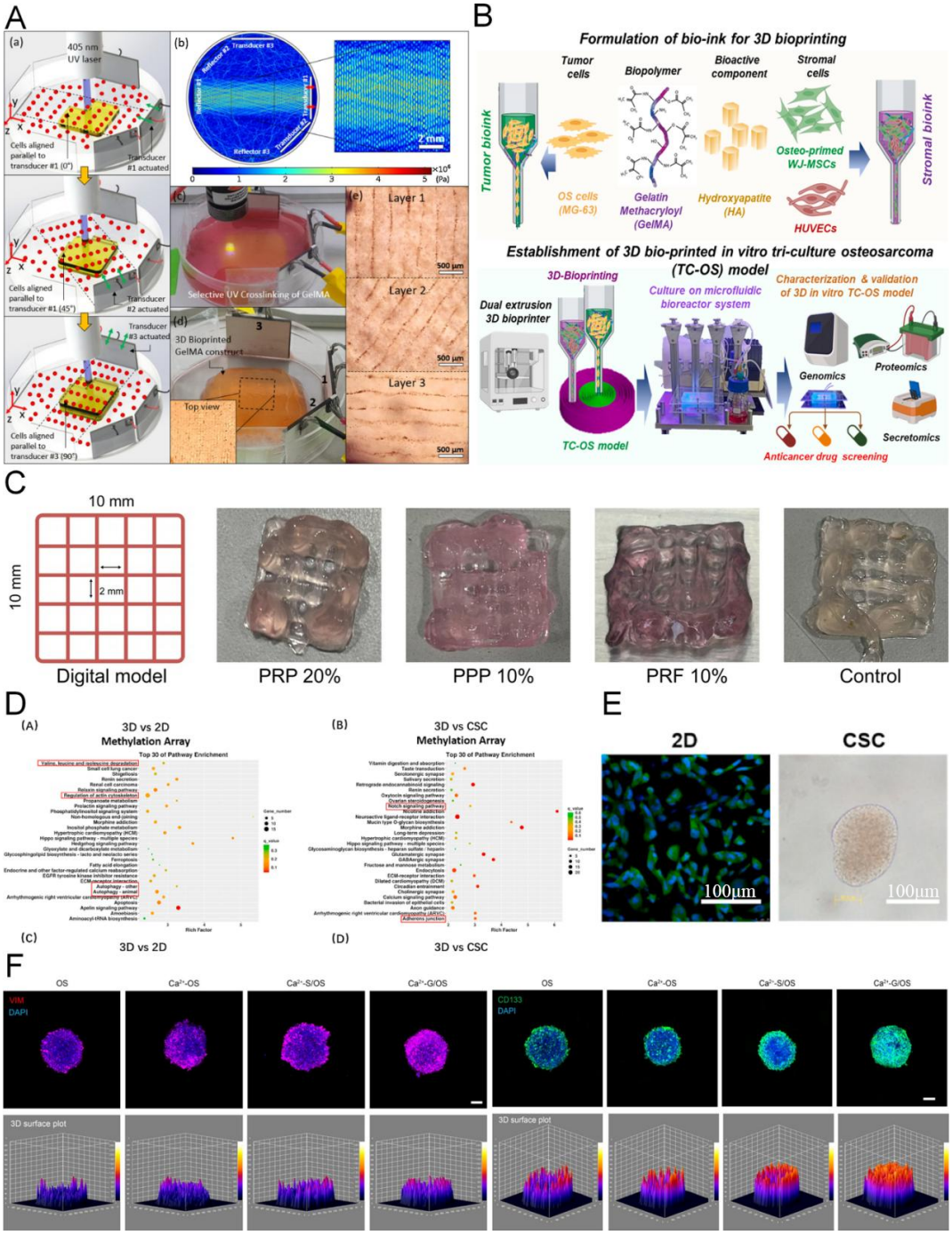

Figure 3. 3D-bioprinted osteosarcoma model. (A) 3D bioprinting of a 3-layer gelatin methacryloyl (GelMA) structure with 0°–45°–90° cell orientations. Reprinted with permission from Chansoria and Shirwaiker.[32] Copyright 2020 ELSEVIER. (B) Schematic of tumor and matrix bioink formulations for 3D bioprinting of each compartment. Reprinted with permission from Jaiswal *et al.*[48] Copyright 2025 ELSEVIER SCI LTD. (C) A digital model of the 10 × 10 × 3 mm construct with a 2 × 2 mm pore architecture. Reprinted with permission from Torres-Ambolumbet *et al.*[51] (D) Transcriptomic data showed that gene expression in 3D-cultured HOS cells differed from that in 2D and cancer stem-like cell (CSC) models. (E) Appearance of 2D monolayer cells (phalloidin-FITC and DAPI staining), tumor spheroids (i.e., CSC), and 3D hydrogel model (HOS). (D–E) Reprinted with permission from Lin *et al.*[34] (F) Immunofluorescence images showing the expression of CD133 and the migration marker VIM in tumor stem cells. Reprinted with permission from Mi *et al.*[49] Copyright 2025 SPRINGER HEIDELBERG.

Abbreviations: DAPI: 4′,6-diamidino-2-phenylindole; FITC: Fluorescein isothiocyanate; HOS: Human osteosarcoma; PPP: Platelet-poor plasma; PRF: Platelet-rich fibrin; PRP: Platelet-rich plasma; VIM: Vimentin.

into multifunctional implants with antibacterial, antioxidant, and tumor-growth–inhibiting properties, heralding an integrated new stage of bone tumor treatment characterized by precise modeling, real-time monitoring, and targeted therapy.

3.1.2. Multiple myeloma

Three-dimensional bioprinting is being used in research on the bone marrow microenvironment in multiple myeloma to reveal the impact of precisely constructed disease-related "niches" on tumor cell survival, proliferation, and drug resistance. By integrating a calcium phosphate cement-based osteogenic microenvironment with a Matrigel-based vascular microenvironment, researchers constructed a dual-subtype niche model, confirming that the vascular microenvironment has a more dominant role than the osteogenic microenvironment in supporting primary myeloma cell proliferation and revealing the differential contributions of the niches to tumor progression.[52] Building on this, coaxial extrusion bioprinting technology further achieved biomimetic precision in structure. By constructing a marrow-like structure with an outer mineralized sheath and an inner soft-gel core, the technology successfully maintained the viability of primary patient cells in vitro for extended periods. This model was also used to validate the enhanced chemosensitivity achieved by interleukin (IL)-6 receptor blockade[53] (Figure 4A and 4C). This evolution from multi-component co-culture to macroscopic structural biomimicry not only provides a high-fidelity platform for analyzing interactions among multiple myeloma cells and the complex bone marrow microenvironment, but also directly promotes the translational application of clinical, individualized drug evaluation and precision therapy.

3.1.3. Acute myeloid leukemia

In the study of bone marrow microenvironment in acute myeloid leukemia (AML), 3D bioprinting technology has shown great potential in simulating disease complexity and accelerating the development of new therapies. A previous study successfully developed an automated robotic bioprinting platform by utilizing a unique self-assembling tetrameric peptide hydrogel[59] (Figure 4B and 4D). This platform, combined with a novel coaxial nozzle technology, enabled the precise construction of an AML 3D bone marrow disease model, allowing controlled deposition of leukemic cells along with bone marrow stromal and endothelial cells, thereby mimicking the spatial architecture of the bone marrow microenvironment. This biomimetic bone marrow microenvironment not only formed a porous structure with nanofiber networks and mechanical properties similar to those of the bone marrow extracellular matrix, but also provided a robust foundation for the compatibility and functional studies of AML cells, both in vitro and in vivo, especially in drug screening and resistance mechanism research. By integrating RNA sequencing and gene expression analysis, this model is expected to provide deeper insights into the drug resistance mechanisms in AML within a complex bone marrow microenvironment and to accelerate the development of novel therapeutic strategies targeting AML relapse and drug resistance.

3.1.4. Bone marrow microenvironment

The application of 3D bioprinting in bone tumor microenvironment research is advancing in two directions: from precise structural reconstruction to functional simulation and clinical translatability. Firstly, by finely tuning the composite ratio of methylcellulose and alginate, researchers have successfully reconstructed the rheological and ultrastructural characteristics of perivascular bone marrow. This platform can simultaneously maintain the long-term survival of key microenvironmental cells (mesenchymal stem cells and endothelial cells) and induce spontaneous dedifferentiation of breast cancer cells to acquire cancer stem cell characteristics, deeply revealing the specific mechanisms by which the bone marrow microenvironment drives tumor cell drug resistance and recurrence.[143] Building upon this, the novel DeepFreeze 3D cryobioprinting technology has overcome the bottlenecks of traditional 3D printing in thick-tissue manufacturing, cell viability maintenance, and long-term storage. Through layer-by-layer cryo-consolidation and dECM composite, the printed bone-like constructs can achieve centimeter-scale mass production, long-term cryopreservation, and rapid functional recovery after thawing[29] (Figure 4F). This transforms bone tumor microenvironment models from "disposable research tools" in the laboratory into "off-the-shelf medical models" that can be mass-produced, inventoried, and repeatedly used.

3.2. Secondary bone tumors

3.2.1. Breast cancer

In the realm of microenvironment simulation, 3D bioprinting has achieved a transition from single-component modeling to the reproduction of complex pathological processes. Early research focused on establishing the interactive inhibitory and promotive relationship between tumor cells and osteoblasts/mesenchymal stem cells through a composite of GelMA and nHA.[54] Subsequently, innovations in bio-inks introduced anisotropic fibrous microgels (μRB), which induced oriented cell alignment via physical topological cues, simulating more realistic tissue heterogeneity[22]

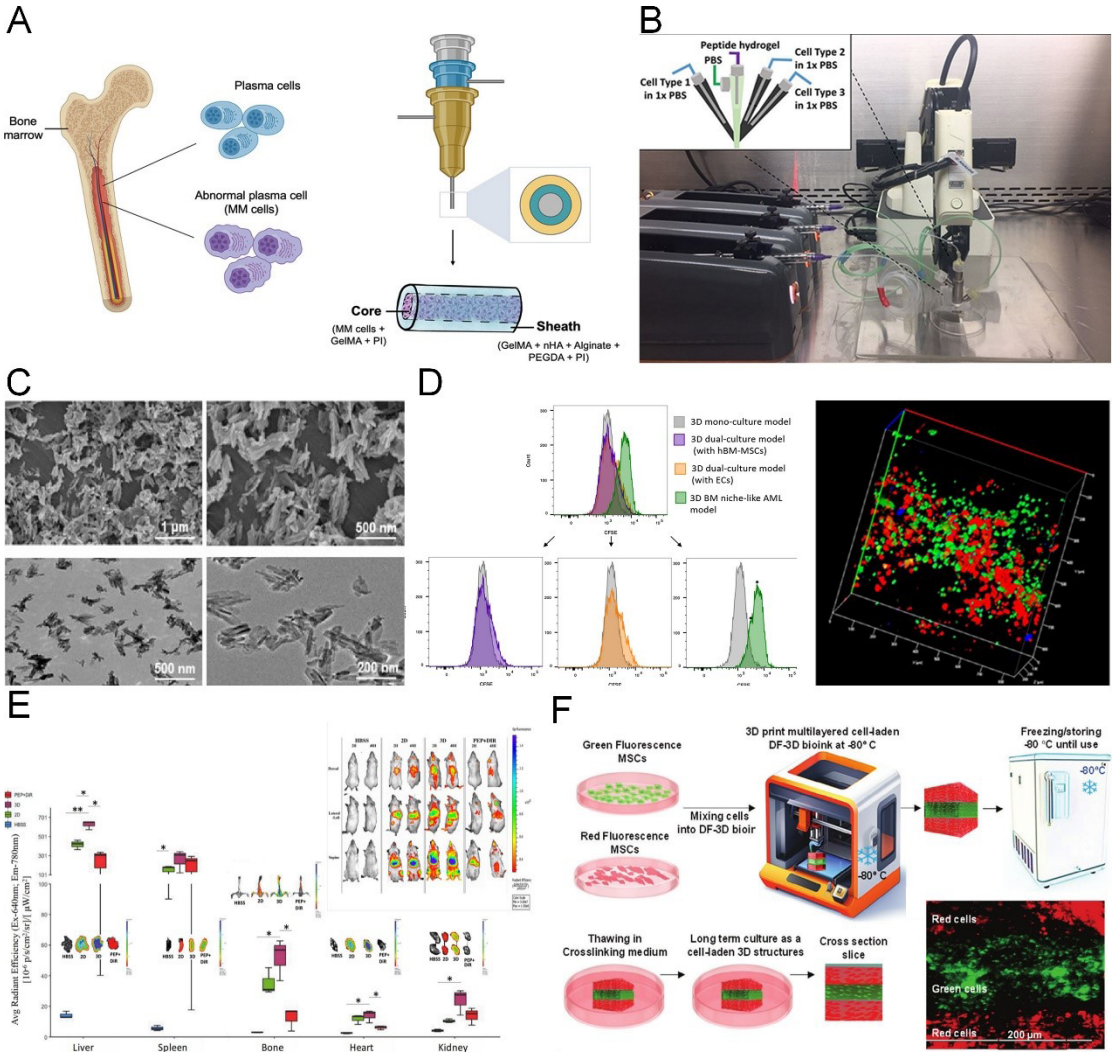

Figure 4. 3D bioprinting of multiple myeloma and bone marrow microenvironment models. (A) Multiple myeloma in vitro high-content modeling using coaxial bioprinting. Reprinted with permission from Wu *et al.*[53] Copyright 2022 WILEY. (B) Robotic 3D bioprinting system with a novel quadruple coaxial nozzle design and microfluidic syringe pump. Fluorescence-labeled multicellular printing. Reprinted with permission from Alhattab *et al.*[59] (C) Scanning electron microscopy (top) and transmission electron microscopy (bottom) images of the nHA. Reprinted with permission from Wu *et al.*[53] Copyright 2022, WILEY. (D). Effect of 3D cell culture conditions on KG1a cell proliferation and fluorescence-labeled multicellular printing. (E) In vivo fluorescence imaging of mice after receiving DIR-stained KG1a cells from 2D or 3D models. (D–E) Reprinted with permission from Alhattab *et al.*[59] (F) DeepFreeze (DF)-3D bioink mixed with GFP Tu167 cells or red fluorescent dye-stained MSCs, followed by DF-3D bioprinting and storage at −80 °C for 24 h. Reprinted with permission from Kumar *et al.*[29]

Abbreviations: DIR: 1,1′-dioctadecyl-3,3,3′,3′-tetramethylindotricarbocyanine iodide; GelMA: Gelatin methacryloyl; nHA: Nanohydroxyapatite; PBS: Phosphate-buffered saline; PEGDA: Polyethylene glycol diacrylate; PI: Photoinitiator.

(Figure 5B and 5C). Further development has evolved into integrated platforms that use gradient-stiffness inks such as collagen methacrylate and HAMA in conjunction with microfluidic technology to construct a three-in-one model encompassing the primary tumor site, circulating vasculature, and bone colonization region. This model successfully captured the dynamic evolution of cancer cells from undergoing EMT to extravasation and colonization.[55]

At the level of clinical diagnosis and treatment evaluation, bioprinting platforms have shifted from basic theoretical validation to high-fidelity drug screening and novel therapy assessment. The tumor–vasculature–bone co-culture scaffold constructed via one-step printing not only recreates the cancer cell invasion pathway but also confirms that the 3D microenvironment endows tumor cells with enhanced drug resistance, providing a

more physiologically relevant *in vitro* evaluation system for developing precision anticancer drugs[57] (Figure 5D and 5E). Furthermore, this highly biomimetic co-culture model has also been used to evaluate cutting-edge therapies. For instance, research has demonstrated that cold atmospheric plasma can selectively kill breast cancer cells within the printed scaffold through oxidative stress while protecting surrounding healthy bone matrix cells[56] (Figure 5A). This signifies that 3D bioprinting is not only a key to understanding bone tumor biology but also a crucial technology platform for achieving precise pre-assessment of individualized, non-invasive treatment strategies.

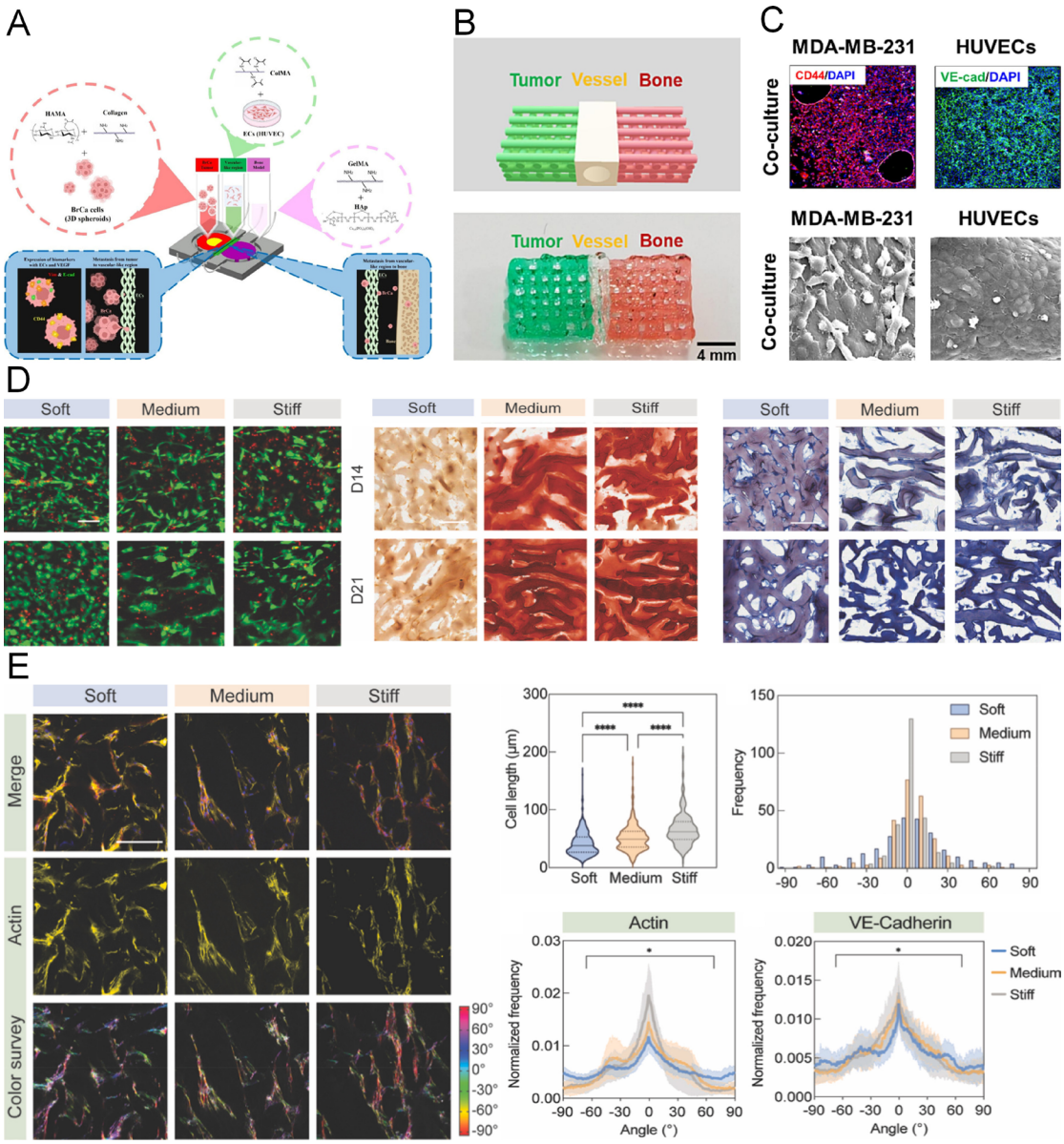

Figure 5. 3D-bioprinted breast cancer bone metastasis model. (A) Schematic diagram of breast cancer metastasis on 3D-bioprinted cancer-on-a-chip. Reprinted with permission from Chang *et al.*[56] (B) Computer-aided design (CAD) diagram and photograph of the co-culture model. (C) Representative images of immunofluorescence staining for MDAMB-231, HUVEC, and OCN, and scanning electron microscopy images of 3D-bioprinted co-culture scaffolds after 14 days of culture. Reprinted with permission from Cheng *et al.*[22] Copyright 2023 ELSEVIER SCIENCE SA. (D) Live/dead staining, alizarin red S (ARS) staining, and aniline blue staining of mesenchymal stem cells (MSCs) after extrusion (day 0) or after 28 days of culture in osteogenic medium. (E) Confocal images of F-actin staining of cell morphology and Vascular endothelial (VE)-cadherin staining of endothelial cell junctions, along with MSC length distribution. Reprinted with permission from Lee *et al.*[57]
Abbreviations: HUVEC: Human umbilical vein endothelial cell; OCN: Osteocalcin.

3.2.2. Prostate cancer

In biological research on prostate cancer bone metastasis, 3D bioprinting and biomimetic microenvironment construction techniques are emerging as key approaches to overcome therapeutic resistance. A previous study successfully constructed a highly biomimetic 3D bone-like microenvironment (a biomimetic bone niche) by cleverly integrating calcium phosphate scaffolds, dECM, and MSCs with osteoblasts[58] (Figure 6). This innovative platform not only induced prostate cancer cells into a clinically relevant state of suppressed proliferation but also exhibited transcriptome characteristics highly consistent with patient-derived single-cell RNA sequencing data, significantly improving the physiological relevance of the in vitro model. More importantly, tumor cells in this biomimetic niche displayed resistance to enzalutamide, accompanied by metabolic reprogramming and activation of pro-survival signaling pathways. The work profoundly revealed the driving role of the bone microenvironment in prostate cancer resistance, providing a crucial and clinically predictive research tool for developing novel therapies targeting drug-resistant tumor states and marking a significant step forward for 3D construction technology in elucidating mechanisms of prostate cancer bone metastasis and in drug screening.

4. Limitations and challenges

Despite rapid progress, current 3D-bioprinted bone tumor models still face several technical and translational bottlenecks that limit their robustness, generalizability, and predictive value. First, reproducibility remains a major concern because bioprinting outcomes are highly sensitive to both material- and process-related variables. Bioink composition (polymer type and concentration, degree of functionalization, crosslinking kinetics), cell handling (viability, density, aggregation state), printing parameters (nozzle size, shear stress, extrusion rate), and post-processing (crosslinking method, time, and intensity) can all shift gelation behavior and cell microenvironments, leading to inter-batch variability. Even when protocols are well described, small deviations in viscosity, temperature, pH, or ionic strength can change printing fidelity and resulting mechanical/transport properties, making cross-study comparisons difficult.

Second, scalability and manufacturability are constrained by the throughput and complexity of living constructs. Many models are produced as small benchtop constructs with carefully optimized geometries; however, translating to clinically relevant sizes requires overcoming limitations in nutrient/oxygen diffusion, cell survival during fabrication, and the ability to maintain desired spatial gradients throughout thicker tissue volumes. Multi-material printing further increases workflow complexity and demands stable interfaces between inks while preserving long-term structural and biological stability. Additionally, long-term culture requirements (media exchange, monitoring, and repeated readouts) can introduce operational variability and can be challenging to standardize for large-scale studies.

Third, vascularization and immune integration remain difficult to recapitulate in a controlled and functional manner. In most existing models, embedded cells rely on diffusion for oxygen and nutrients, which restricts viable tissue thickness and delays mature remodeling processes. While strategies such as incorporating endothelial cells, prevascular networks, or co-cultures have been explored, achieving reliable perfusable vasculature with realistic flow, permeability, and immune cell trafficking remains uncommon. Without vascular and immune functionality, model readouts may not fully reflect tumor progression dynamics, treatment response, and the bidirectional crosstalk between tumor, stromal compartments, and host defenses.

Fourth, the gap between in vitro models and in vivo complexity continues to limit translational confidence. Bone tumor progression is shaped by systemic factors (circulating cytokines and immune mediators, hormonal and metabolic influences) and a multi-scale microenvironment involving bone remodeling, mineralization, extracellular matrix turnover, and mechanical loading. Many bioprinted models emphasize one or a subset of these features-such as extracellular matrix composition, tumor cell spatial organization, or simplified immune/stromal components-while omitting the broader physiological context. As a result, models may capture certain phenotypes (e.g., invasion morphology or chemosensitivity trends) yet fail to reproduce other critical aspects such as metastatic niche formation, vascular–immune coevolution, and long-term treatment-induced remodeling.

Fifth, regulatory and translational hurdles pose additional challenges for clinical translation. For therapeutic-grade applications, materials must meet stringent requirements for safety, purity, and consistency, while manufacturing processes must demonstrate validated control over critical quality attributes (e.g., mechanical properties, crosslinking completeness, degradation behavior, and residual reactants). Even for research models, the increasing use of functionalized polymers (e.g., photocrosslinkable or chemically modified networks) raises concerns about batch consistency, potential cytotoxicity, and the need for standardized characterization

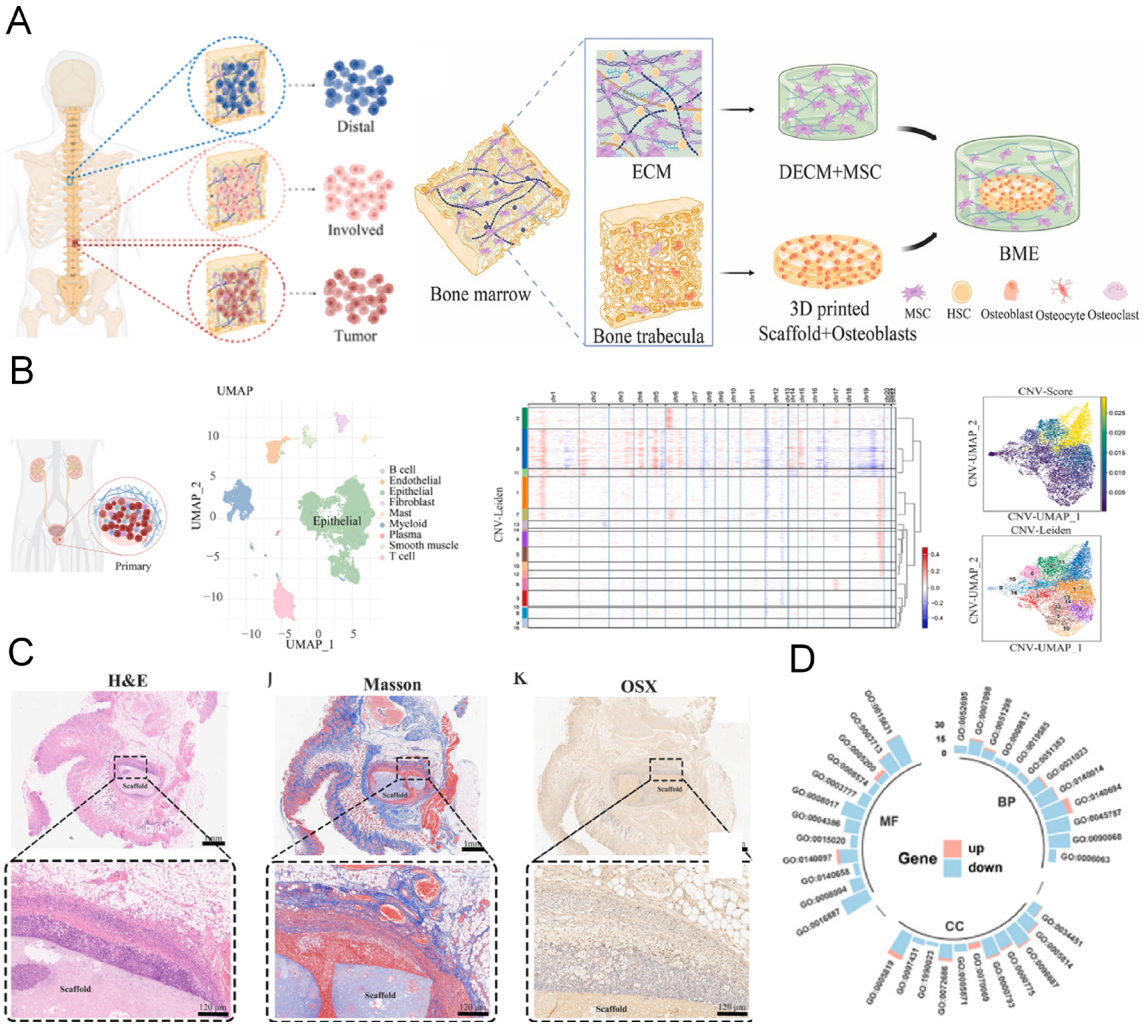

Figure 6. 3D-bioprinted prostate cancer bone metastasis model. (A) Tumor cells were classified into three subpopulations based on their anatomical origin: distal sites, involved sites, and metastatic tumor sites. (B) Single-cell transcriptomic projections of primary tumor cells from 11 patients who underwent radical prostatectomy (left) and a UMAP plot of epithelial cells from radical prostatectomy tissue (right). (C) BME model images at 7 and 28 days post-implantation. (D) GSEA showed downregulation of GO terms related to mitosis and proliferation in the BME. Reprinted with permission from Chen *et al.*[58]

Abbreviations: BME: Bone microenvironment; BP: Biological process; CC: Cellular component; DECM: Decellularized extracellular matrix; ECM: Extracellular matrix; GSEA: Gene set enrichment analysis; H&E: Hemoxylin and eosin; HSC: Hematopoietic stem cell; MF: Molecular function; MSC: Mesenchymal stem cell; OSX: Osterix; UMAP: Uniform manifold approximation and projection.

methods. Furthermore, the path from a promising in vitro platform to an accepted clinical or decision-support tool requires not only biological relevance but also standardized performance criteria, validated endpoints, and evidence that the model meaningfully improves prediction over existing benchmarks.

5. Conclusion

This article systematically reviews and deeply analyzes the latest advancements in constructing bone tumor organoid models using advanced 3D bioprinting technology and their potential applications in tumor research. It begins by outlining the significant challenges in diagnosing and treating bone tumors, particularly primary bone tumors and metastatic bone disease. Building upon this foundation, we focused on how 3D bioprinting, as an innovative technology, can construct highly biomimetic and physiologically relevant bone tumor models by precisely controlling the spatial distribution of biomaterials and biological units. We then summarized its potential applications in elucidating tumor development mechanisms, drug screening and optimization, and the

development of individualized treatment plans.

Three-dimensional bioprinting technology has shown notable potential for constructing bone tumor models, primarily due to its capability to achieve computer-aided, layer-by-layer deposition of cells, growth factors, and biomaterials in 3D. Under appropriately optimized bioink formulations and printing parameters, this approach can generate organoid-like constructs that may better capture aspects of the in vivo tumor microenvironment than conventional 2D models. Bioprinted bone tumor models can be engineered to represent tumor heterogeneity, including cell morphology, spatial arrangement, and phenotypic behaviors such as proliferation, migration, and invasion, as well as cell–cell and cell–extracellular matrix interactions. In addition, compared with traditional experimental systems, bioprinted platforms *may* provide more relevant contexts for evaluating drug efficacy and toxicity, potentially reducing some bias arising from physiological differences. Moreover, features such as scalability, batch-to-batch consistency, and the possibility of constructing patient-derived models have been explored for drug screening and precision medicine-oriented research; however, these advantages are still largely dependent on standardization of printing workflows, validation of construct maturation, and systematic assessment of reproducibility and physiological relevance. Therefore, while bioprinting represents a promising experimental route, it remains at an evolving stage, and practical limitations (e.g., material availability, crosslinking constraints, imaging/characterization requirements, and translational scalability) need further resolution before broad clinical translation.

To address the unique physiological complexity of bone, future 3D bioprinting efforts must transition from basic structural replication to the precise reconstruction of the mineralized matrix and the "vicious cycle" microenvironment. Specifically, the field should prioritize the development of gradient bioinks incorporating hydroxyapatite to mimic bone's mechanical hierarchy, alongside multi-cellular printing strategies that integrate osteoclasts, osteoblasts, and sensory nerves to capture bone-specific tumor progression and pain mechanisms. Practically, the integration of dynamic perfusion bioreactors to simulate bone marrow hemodynamics and the use of patient-derived cells for high-throughput drug-sensitivity screening will be pivotal. This targeted evolution will transform 3D-bioprinted bone tumor models from descriptive research tools into high-fidelity, predictive platforms, providing clear guidance for personalized therapy and mechanistic discovery in primary and metastatic bone malignancies.

Acknowledgments

None.

Funding

This work was supported by the Liaoning Provincial Department of Education Project (JYTMS20231829) and the Liaoning Provincial Department of Science and Technology Project (2023-MSLH-157).

Conflict of interest

The authors declare that they have no known competing financial interests or personal relationships that could have appeared to influence the work reported in this paper.

Author contributions

Conceptualization: Xinghong Sun
Supervision: Xinghong Sun
Visualization: Miao Wang
Writing–original draft: Miao Wang
Writing–review & editing: Tingyao Zang, Xinghong Sun, Xiangran Cui, Ning Wang

Ethics approval and consent to participate

Not applicable.

Consent for publication

Not applicable.

Availability of data

Not applicable.

References

1. von Eisenhart-Rothe R, Toepfer A, Salzmann M, Schauwecker J, Gollwitzer H, Rechl H. Primary malignant bone tumors. *Orthopade*. 2011;40(12):1121-1139.

   doi: 10.1007/s00132-011-1866-7

2. Guan YJ, Zhang W, Mao YL, Li SL. Nanoparticles and bone microenvironment: a comprehensive review for malignant bone tumor diagnosis and treatment. *Mol Cancer*. 2024;23(1):246.

   doi: 10.1186/s12943-024-02161-1

3. Aldashash F, Elraie M. Solitary osteochondroma of the proximal femur causing sciatic nerve compression. *Ann Saudi Med*. 2017;37(2):166-169.

   doi: 10.5144/0256-4947.2017.166

4. Wewel JT, O'Toole JE. Epidemiology of spinal cord and column tumors. *Neuro-Oncol Pract*. 2020;7:5-9.

   doi: 10.1093/nop/npaa046

5. Kang YB. Dissecting Tumor-Stromal Interactions in Breast Cancer Bone Metastasis. *Endocr Metab*. 2016;31(2):206-212.

   doi: 10.3803/EnM.2016.31.2.206

6. Wang XX, Zhang TJ, Zheng BX, *et al*. Lymphotoxin-β promotes breast cancer bone metastasis colonization and osteolytic outgrowth. *Nat Cell Biol*. 2024;26(9):1597-1612.

   doi: 10.1038/s41556-024-01478-9

7. Yang HB, Yu ZY, Ji SS, *et al*. Targeting bone microenvironments for treatment and early detection of cancer bone metastatic niches. *J Control Release*. 2022;341:443-456.

   doi: 10.1016/j.jconrel.2021.11.005

8. Liu WH, Zhao Y, Liu ZF, *et al*. Therapeutic effects against high-grade glioblastoma mediated by engineered induced neural stem cells combined with GD2-specific CAR-NK. *Cell Oncol*. 2023;46(6):1747-1762.

   doi: 10.1007/s13402-023-00842-5

9. Zhao HR, Bao SY, Chen SL, *et al*. Phytosomes Loaded with Mastoparan-M Represent a Novel Strategy for Breast Cancer Treatment. *Int J Nanomedicine*. 2025;20:109-124.

   doi: 10.2147/ijn.S481871

10. Chen SS, Chen W, Guan ZY, *et al*. Development of a 3D-3 co-culture microbead consisting of cancer-associated fibroblasts and human umbilical vein endothelial cells for the anti-tumor drug assessment of lung cancer. *Transl Lung Cancer Res*. 2025;14(6):2159-2179.

    doi: 10.21037/tlcr-2025-525

11. Deng Y, Chen QY, Yang X, *et al*. Tumor cell senescence-induced macrophage CD73 expression is a critical metabolic immune checkpoint in the aging tumor microenvironment. *Theranostics*. 2024;14(3):1224-1240.

    doi: 10.7150/thno.91119

12. Hung HC, Mao TL, Fan MH, *et al*. Enhancement of Tumorigenicity, Spheroid Niche, and Drug Resistance of Pancreatic Cancer Cells in Three-Dimensional Culture System. *J Cancer*. 2024;15(8):2292-2305.

    doi: 10.7150/jca.87494

13. Zhang ZY, Chen XB, Gao SJ, Fang XD, Ren SN. 3D bioprinted tumor model: a prompt and convenient platform for overcoming immunotherapy resistance by recapitulating the tumor microenvironment. *Cell Oncol*. 2024;47(4):1113-1126.

    doi: 10.1007/s13402-024-00935-9

14. Haddad AF, Young JS, Amara D, *et al*. Mouse models of glioblastoma for the evaluation of novel therapeutic strategies. *Neuro-Oncol Adv*. 2021;3(1).

    doi: 10.1093/noajnl/vdab100

15. Pu FF, Guo HY, Shi DY, *et al*. The generation and use of animal models of osteosarcoma in cancer research. *Genes Dis*. 2024;11(2):664-674.

    doi: 10.1016/j.gendis.2022.12.021

16. DiMarco AV, Maddalo D. In Vivo Modeling of Tumor Heterogeneity for Immuno-Oncology Studies: Failures, Improvements, and Hopes. *Curr Protoc*. 2022;2(3):e377.

    doi: 10.1002/cpz1.377

17. Jardim-Perassi BV, Alexandre PA, Sonehara NM, *et al*. RNA-Seq transcriptome analysis shows anti-tumor actions of melatonin in a breast cancer xenograft model. *Sci Rep*. 2019;9:966.

    doi: 10.1038/s41598-018-37413-w

18. Fischetti T, Di Pompo G, Baldini N, Avnet S, Graziani G. 3D Printing and Bioprinting to Model Bone Cancer: The Role of Materials and Nanoscale Cues in Directing Cell Behavior. *Cancers*. 2021;13(16):4065.

    doi: 10.3390/cancers13164065

19. Ortega MA, De Leon-Oliva D, Boaru DL, *et al*. Advances in 3D bioprinting to enhance translational applications in bone tissue engineering and regenerative medicine. *Histol Histopathol*. 2025;40(2):147-156.

    doi: 10.14670/hh-18-763

20. Samadian H, Jafari S, Sepand MR, *et al*. 3D bioprinting technology to mimic the tumor microenvironment: tumor-on-a-chip concept. *Mater Today Adv*. 2021;12:100160.

    doi: 10.1016/j.mtadv.2021.100160

21. Vrana NE, Gupta S, Mitra K, *et al*. From 3D printing to 3D bioprinting: the material properties of polymeric material and its derived bioink for achieving tissue specific architectures. *Cell Tissue Bank*. 2022;23(3):417-440.

    doi: 10.1007/s10561-021-09975-z

22. Cheng SN, Li YX, Yu CG, Deng ZW, Huang J, Zhang ZJ. 3D bioprinted tumor-vessel-bone co-culture scaffold for breast cancer bone metastasis modeling and drug testing. *Chem Eng J*. 2023;476:146685.

    doi: 10.1016/j.cej.2023.146685

23. Pragnere S, Essayan L, El-Kholti N, Petiot E, Pailler-Mattei C. In vitro bioprinted 3D model enhancing osteoblast-to-osteocyte differentiation. *Biofabrication*. 2025;17(1):015021.

    doi: 10.1088/1758-5090/ad8ca6

24. Singh YP, Moses JC, Bandyopadhyay A, Mandal BB. 3D Bioprinted Silk-Based In Vitro Osteochondral Model for Osteoarthritis Therapeutics. *Adv Healthc Mater*. 2022;11(24):2200209.

    doi: 10.1002/adhm.202200209

25. Hu QX, Wang YH, Song YT, Liu SH, Zhang HG. Engineering triple-layer gelatin methacryloyl-alginate osteochondral construct with biomimetic curved architecture using a multi-axial, multi-process, multi-material 3D bioprinting

system. *Int J Biol Macromol*. 2025;327:147541.

doi: 10.1016/j.ijbiomac.2025.147541

26. Khobragade SS, Deshmukh M, Vyas U, Ingle RG. Innovative Approaches in Bone Tissue Engineering: Strategies for Cancer Treatment and Recovery. *Int J Mol Sci*. 2025;26(9):3937.

doi: 10.3390/ijms26093937

27. Domingues MF, Carreira MC, Santos MS, *et al*. A 3D Bioprinted Spheroid-Laden dECM-Enriched Osteosarcoma Model for Enhanced Drug Testing and Therapeutic Discovery. *Adv Healthc Mater*. 2026;15(15).

doi: 10.1002/adhm.202503633

28. Dutta SD, Patil TV, Ganguly K, Randhawa A, Lim KT. Unraveling the potential of 3D bioprinted immunomodulatory materials for regulating macrophage polarization: State-of-the-art in bone and associated tissue regeneration. *Bioact Mater*. 2023;28:284-310.

doi: 10.1016/j.bioactmat.2023.05.014

29. Kumar A, Brown RA, Roufaeil DB, *et al*. DeepFreeze 3D-biofabrication for Bioengineering and Storage of Stem Cells in Thick and Large-Scale Human Tissue Analogs. *Adv Sci*. 2024;11(11).

doi: 10.1002/advs.202306683

30. Rehovsky C, Bajwa DS, Mallik S, Pullan JE, Ara I. Natural polymer hydrogel based 3D printed bioreactor testing platform for cancer cell culture. *Mater Today Commun*. 2024;39:108925.

doi: 10.1016/j.mtcomm.2024.108925

31. Vakhrushev IV, Nezhurina EK, Karalkin PA, *et al*. Heterotypic Multicellular Spheroids as Experimental and Preclinical Models of Sprouting Angiogenesis. *Biology*. 2022;11(1):18.

doi: 10.3390/biology11010018

32. Chansoria P, Shirwaiker R. 3D bioprinting of anisotropic engineered tissue constructs with ultrasonically induced cell patterning. *Addit Manuf*. 2020;32:101042.

doi: 10.1016/j.addma.2020.101042

33. Chen Y, Xiong X, Liu X, *et al*. 3D Bioprinting of shear-thinning hybrid bioinks with excellent bioactivity derived from gellan/alginate and thixotropic magnesium phosphate-based gels. *J Mater Chem B*. 2020;8(25):5500-5514.

doi: 10.1039/d0tb00060d

34. Lin YX, Yang YQ, Yuan K, *et al*. Multi-omics analysis based on 3D-bioprinted models innovates therapeutic target discovery of osteosarcoma. *Bioact Mater*. 2022;18:459-470.

doi: 10.1016/j.bioactmat.2022.03.029

35. Pellegrini E, Desando G, Petretta M, *et al*. A 3D Collagen-Based Bioprinted Model to Study Osteosarcoma Invasiveness and Drug Response. *Polymers*. 2022;14(19):4070.

doi: 10.3390/polym14194070

36. Pant S, Thomas S, Loganathan S, Valapa RB. 3D bioprinted poly(lactic acid)/mesoporous bioactive glass based biomimetic scaffold with rapid apatite crystallization and in-vitro Cytocompatability for bone tissue engineering. *Int J Biol Macromol*. 2022;217:979-997.

doi: 10.1016/j.ijbiomac.2022.07.202

37. Zhu H, Monavari M, Zheng K, *et al*. 3D Bioprinting of Multifunctional Dynamic Nanocomposite Bioinks Incorporating Cu-Doped Mesoporous Bioactive Glass Nanoparticles for Bone Tissue Engineering. *Small*. 2022;18(12):2104996.

doi: 10.1002/smll.202104996

38. Loi G, Stucchi G, Scocozza F, *et al*. Characterization of a Bioink Combining Extracellular Matrix-like Hydrogel with Osteosarcoma Cells: Preliminary Results. *Gels*. 2023;9(2):129.

doi: 10.3390/gels9020129

39. Liang J, Wang ZL, Poot AA, Grijpma DW, Dijkstra PJ, Wang R. Enzymatic post-crosslinking of printed hydrogels of methacrylated gelatin and tyramine-conjugated 8-arm poly(ethylene glycol) to prepare interpenetrating 3D network structures. *Int J Bioprint*. 2023;9(5):522-537.

doi: 10.18063/ijb.750

40. Lin YX, Yuan K, Yang YQ, *et al*. Osteosarocma progression in biomimetic matrix with different stiffness: Insights from a three-dimensional printed gelatin methacrylamide hydrogel. *Int J Biol Macromol*. 2023;252:126391.

doi: 10.1016/j.ijbiomac.2023.126391

41. Shi YW, Wang ZZ, Zhou XT, *et al*. Preparation of a 3D printable high-performance GelMA hydrogel loading with magnetic cobalt ferrite nanoparticles. *Front Bioeng Biotechnol*. 2023;11:1132192.

doi: 10.3389/fbioe.2023.1132192

42. Delgrosso E, Scocozza F, Cansolino L, *et al*. 3D bioprinted osteosarcoma model for experimental boron neutron capture therapy (BNCT) applications: Preliminary assessment. *J Biomed Mater Res B Appl Biomater*. 2023;111(8):1571-1580.

doi: 10.1002/jbm.b.35255

43. Julson JR, Horton SC, Quinn CH, *et al*. CDK4/6 Inhibition With Lerociclib is a Potential Therapeutic Strategy for the Treatment of Pediatric Sarcomas. *J Pediatr Surg*. 2024;59(3):473-482.

doi: 10.1016/j.jpedsurg.2023.10.004

44. Anspach A, Bider F, Voelkl AR, Taylor RNK, Boccaccini AR. Incorporating silica nanoparticles with silver patches into alginate-based bioinks for 3D bioprinting. *MRS Commun*. 2024;14(6):1460-1466.

doi: 10.1557/s43579-024-00668-8

45. Bider F, Miola M, Clejanu CE, *et al*. 3D bioprinting of multifunctional alginate dialdehyde (ADA)-gelatin (GEL) (ADA-GEL) hydrogels incorporating ferulic acid. *Int J Biol Macromol*. 2024;257:128449.

doi: 10.1016/j.ijbiomac.2023.128449

46. Chrungoo S, Bharadwaj T, Verma D. Nanofibrous polyelectrolyte complex incorporated BSA-alginate composite bioink for 3D bioprinting of bone mimicking constructs. *Int J Biol Macromol*. 2024;266:131123.

doi: 10.1016/j.ijbiomac.2024.131123

47. Güner E, Yildirim-Semerci O, Altan Z, Arslan-Yildiz A. Peptide-functionalized hydrocolloid bioink for 3D bioprinting in dental tissue engineering. *Int J Biol Macromol*. 2025;330:148016.

doi: 10.1016/j.ijbiomac.2025.148016

48. Jaiswal C, Dey S, Prasad J, Gupta R, Agarwala M, Mandal BB. 3D bioprinted microfluidic based osteosarcoma-on-a chip model as a physiomimetic pre-clinical drug testing platform for anti-cancer drugs. *Biomaterials*. 2025;320:123267.

doi: 10.1016/j.biomaterials.2025.123267

49. Mi XL, Ren Y, Wang HB, *et al*. Bioprinted integrated gradient biomechanical signal-tailored osteosarcoma model: advancing insights into tumor development and drug screening. *Bio-Des Manuf*. 2025;8(3):423-441.

doi: 10.1631/bdm.2400108

50. Fischetti T, Graziani G, Borciani G, *et al*. Development of novel organic/inorganic osteomimetic inks for 3D bioprinted in vitro bone models. *Biomater Adv*. 2026;180:214608.

doi: 10.1016/j.bioadv.2025.214608

51. Torres-Ambolumbet VC, Ocampo-Terreros MS, Anaya-Sampayo LM, García-Robayo DA. Bio-inks with PRF Increase Human Osteosarcoma Cell Line (SaOS-2) Viability in Extrusion-Based 3D-Bioprinted Constructs. *Ann Biomed Eng*. 2026.

doi: 10.1007/s10439-026-04023-x

52. Braham MVJ, Ahlfeld T, Akkineni AR, *et al*. Endosteal and Perivascular Subniches in a 3D Bone Marrow Model for Multiple Myeloma. *Tissue Eng Part C Methods*. 2018;24(5):300-312.

doi: 10.1089/ten.tec.2017.0467

53. Wu D, Wang ZY, Li J, *et al*. A 3D-Bioprinted Multiple Myeloma Model. *Adv Healthc Mater*. 2022;11(7):2100884.

doi: 10.1002/adhm.202100884

54. Zhou X, Zhu W, Nowicki M, *et al*. 3D Bioprinting a Cell-Laden Bone Matrix for Breast Cancer Metastasis Study. *ACS Appl Mater Interfaces*. 2016;8(44):30017-30026.

doi: 10.1021/acsami.6b10673

55. Bouret LM, Billeau JB, Weber MH, Rosenzweig DH, Reuter S. Cold Atmospheric Plasma Selectively Disrupts Breast Cancer Growth in a Bioprinted 3D Tumor-Stroma Co-Culture Model. *Adv Healthc Mater*. 2025;14(28).

doi: 10.1002/adhm.202405292

56. Chang TW, Huang MW, Dong GC, Lee IC. Construction of a 3D Bioprinted Microfluidic Platform to Study Breast Cancer Bone Metastasis and Tumor Microenvironmental Influences. *ACS Appl Mater Interfaces*. 2025;17(45):61718-61730.

doi: 10.1021/acsami.5c15529

57. Lee HP, Tai M, Jones SJ, *et al*. Ribbon-shaped microgels as bioinks for 3D bioprinting of anisotropic tissue structures. *Bioact Mater*. 2026;59:595-606.

doi: 10.1016/j.bioactmat.2025.12.040

58. Chen X, Peng YJ, Zhao Y, *et al*. Biomimetic bone niche reconstructs proliferation-inhibited and therapy-resistant bone-metastatic prostate cancer. *Bioact Mater*. 2026;56:15-32.

doi: 10.1016/j.bioactmat.2025.09.041

59. Alhattab DM, Isaioglou I, Alshehri S, *et al*. Fabrication of a three-dimensional bone marrow niche-like acute myeloid Leukemia disease model by an automated and controlled process using a robotic multicellular bioprinting system. *Biomater Res*. 2023;27(1):111.

doi: 10.1186/s40824-023-00457-9

60. Ng WL, Shkolnikov V. Optimizing cell deposition for inkjet-based bioprinting. *Int J Bioprint*. 2024;10(2):182-206.

doi: 10.36922/ijb.2135

61. Zhao DK, Xu HQ, Yin J, Yang HY. Inkjet 3D bioprinting for tissue engineering and pharmaceutics. *J Zhejiang Univ Sci A*. 2022;23(12):955-973.

doi: 10.1631/2023.A2200569

62. Takagi D, Lin W, Matsumoto T, *et al*. High-precision three-dimensional inkjet technology for live cell bioprinting. *Int J Bioprint*. 2019;5(2):27-38.

doi: 10.18063/ijb.v5i2.208

63. Zhu HX, Li R, Li S, *et al*. Multi-physical field control piezoelectric inkjet bioprinting for 3D tissue-like structure manufacturing. *Int J Bioprint*. 2024;10(3):359-378.

doi: 10.36922/ijb.2120

64. Wan WM, Wang X, Zhang RT, *et al*. Construction of artificial lung tissue structure with 3D-inkjet bioprinting core for pulmonary disease evaluation. *J Tissue Eng*. 2025;16:20417314251328128.

doi: 10.1177/20417314251328128

65. Zhang SK, Chen X, Shan MY, *et al*. Convergence of 3D Bioprinting and Nanotechnology in Tissue Engineering

Scaffolds. *Biomimetics*. 2023;8(1):94.

doi: 10.3390/biomimetics8010094

66. Kacarevic ZP, Rider PM, Alkildani S, *et al*. An Introduction to 3D Bioprinting: Possibilities, Challenges and Future Aspects. *Materials*. 2018;11(11):2199.

doi: 10.3390/ma11112199

67. de Barros NR, Harb SV, Horinouchi CDD, *et al*. Advances in 3D Bioprinting and Microfluidics for Organ-on-a-Chip Platforms. *Polymers*. 2025;17(22):3078.

doi: 10.3390/polym17223078

68. Yang S, Tang H, Feng CM, Shi JP, Yang JQ. The Research on Multi-Material 3D Vascularized Network Integrated Printing Technology. *Micromachines*. 2020;11(3):237.

doi: 10.3390/mi11030237

69. Dufour A, Gallostra XB, O'Keeffe C, *et al*. Integrating melt electrowriting and inkjet bioprinting for engineering structurally organized articular cartilage. *Biomaterials*. 2022;283:121405.

doi: 10.1016/j.biomaterials.2022.121405

70. Hedegaard CL, Collin EC, Redondo-Gómez C, *et al*. Hydrodynamically Guided Hierarchical Self-Assembly of Peptide-Protein Bioinks. *Adv Funct Mater*. 2018;28(16):1703716.

doi: 10.1002/adfm.201703716

71. Daly AC, Kelly DJ. Biofabrication of spatially organised tissues by directing the growth of cellular spheroids within 3D printed polymeric microchambers. *Biomaterials*. 2019;197:194-206.

doi: 10.1016/j.biomaterials.2018.12.028

72. Li JF, Fischer P. Advances in extrusion-based bioprinting enabled by advanced printhead and nozzle designs. *Mater Today Bio*. 2026;37:102941.

doi: 10.1016/j.mtbio.2026.102941

73. Placone JK, Engler AJ. Recent Advances in Extrusion-Based 3D Printing for Biomedical Applications. *Adv Healthc Mater*. 2018;7(8):1701161.

doi: 10.1002/adhm.201701161

74. Li XR, Zheng FY, Wang XD, *et al*. Biomaterial inks for extrusion-based 3D bioprinting: Property, classification, modification, and selection. *Int J Bioprint*. 2023;9(2):649.

doi: 10.18063/ijb.v9i2.649

75. Moon SH, Park TY, Cha HJ, Yang YJ. Photo-/thermo-responsive bioink for improved printability in extrusion-based bioprinting. *Mater Today Bio*. 2024;25:100973.

doi: 10.1016/j.mtbio.2024.100973

76. Bakirci E, Adib AA, Ashraf SF, Feinberg AW. Advancing extrusion-based embedded 3D bioprinting via scientific, engineering, and process innovations. *Biofabrication*. 2025;17(2):023002.

doi: 10.1088/1758-5090/adb7c3

77. Naghieh S, Chen XB. Printability-A key issue in extrusion-based bioprinting. *J Pharm Anal*. 2021;11(5):564-579.

doi: 10.1016/j.jpha.2021.02.001

78. Li H, Li NN, Zhang H, *et al*. Three-Dimensional Bioprinting of Perfusable Hierarchical Microchannels with Alginate and Silk Fibroin Double Cross-linked Network. *3D Print Addit Manuf*. 2020;7(2):78-84.

doi: 10.1089/3dp.2019.0115

79. Mohan TS, Datta P, Nesaei S, Ozbolat V, Ozbolat IT. 3D coaxial bioprinting: process mechanisms, bioinks and applications. *Prog Biomed Eng*. 2022;4(2):022003.

doi: 10.1088/2516-1091/ac631c

80. Kim JH, Park M, Shim JH, Yun WS, Jin S. Multi-scale vascularization strategy for 3D-bioprinted tissue using coaxial core-shell pre-set extrusion bioprinting and biochemical factors. *Int J Bioprint*. 2023;9(4):ijb726.

doi: 10.18063/ijb.726

81. Wu CA, Zhu YJ, Venkatesh A, Stark CJ, Lee SH, Woo YJ. Optimization of Freeform Reversible Embedding of Suspended Hydrogel Microspheres for Substantially Improved Three-Dimensional Bioprinting Capabilities. *Tissue Eng Part C Methods*. 2023;29(3):85-94.

doi: 10.1089/ten.tec.2022.0214

82. Zhu YJ, Stark CJ, Madira S, *et al*. Three-Dimensional Bioprinting with Alginate by Freeform Reversible Embedding of Suspended Hydrogels with Tunable Physical Properties and Cell Proliferation. *Bioengineering*. 2022;9(12):807.

doi: 10.3390/bioengineering9120807

83. Ghazali HS, Askari E, Ghazali ZS, Naghib SM, Braschler T. Lithography-based 3D printed hydrogels: From bioresin designing to biomedical application. *Colloid Interface Sci Commun*. 2022;50:100667.

doi: 10.1016/j.colcom.2022.100667

84. Liang RJ, Gu YQ, Wu YC, Bunpetch V, Zhang SF. Lithography-Based 3D Bioprinting and Bioinks for Bone Repair and Regeneration. *ACS Biomater Sci Eng*. 2021;7(3):806-816.

doi: 10.1021/acsbiomaterials.9b01818

85. Lim KS, Galarraga JH, Cui XL, Lindberg GCJ, Burdick JA, Woodfield TBF. Fundamentals and Applications of Photo-Cross-Linking in Bioprinting. *Chem Rev*. 2020;120(19):10637-10669.

doi: 10.1021/acs.chemrev.9b00812

86. Dobos A, Van Hoorick J, Steiger W, *et al*. Thiol-Gelatin-Norbornene Bioink for Laser-Based High-Definition

Bioprinting. *Adv Healthc Mater*. 2020;9(15):1900752.

doi: 10.1002/adhm.201900752

87. Lim KS, Levato R, Costa PF, *et al*. Bio-resin for high resolution lithography-based biofabrication of complex cell-laden constructs. *Biofabrication*. 2018;10(3):034101.

doi: 10.1088/1758-5090/aac00c

88. Kim D, Kang D, Kim D, Jang J. Volumetric bioprinting strategies for creating large-scale tissues and organs. *MRS Bull*. 2023;48(6):657-667.

doi: 10.1557/s43577-023-00541-4

89. Lian LM, Xie MB, Luo ZY, *et al*. Rapid Volumetric Bioprinting of Decellularized Extracellular Matrix Bioinks. *Adv Mater*. 2024;36(34).

doi: 10.1002/adma.202304846

90. Gittard SD, Nguyen A, Obata K, Koroleva A, Narayan RJ, Chichkov BN. Fabrication of microscale medical devices by two-photon polymerization with multiple foci via a spatial light modulator. *Biomed Opt Express*. 2011;2(11):3167-3178.

doi: 10.1364/boe.2.003167

91. Zhang YS, Su YM, Zhao Y, Wang ZY, Wang C. Two-Photon 3D Printing in Metal-Organic Framework Single Crystals. *Small*. 2022;18(18):2200514.

doi: 10.1002/smll.202200514

92. Grigoryan B, Sazer DW, Avila A, *et al*. Development, characterization, and applications of multi-material stereolithography bioprinting. *Sci Rep*. 2021;11(1):3171.

doi: 10.1038/s41598-021-82102-w

93. Thomas A, Orellano I, Lam T, *et al*. Vascular bioprinting with enzymatically degradable bioinks via multi-material projection-based stereolithography. *Acta Biomater*. 2020;117:121-132.

doi: 10.1016/j.actbio.2020.09.033

94. Li XD, Liu BX, Pei B, *et al*. Inkjet Bioprinting of Biomaterials. *Chem Rev*. 2020;120(19):10596-10636.

doi: 10.1021/acs.chemrev.0c00008

95. Gao Q, He Y, Fu JZ, Liu A, Ma L. Coaxial nozzle-assisted 3D bioprinting with built-in microchannels for nutrients delivery. *Biomaterials*. 2015;61:203-215.

doi: 10.1016/j.biomaterials.2015.05.031

96. Kim SH, Yeon YK, Lee JM, *et al*. Precisely printable and biocompatible silk fibroin bioink for digital light processing 3D printing. *Nat Commun*. 2018;9(1):1620.

doi: 10.1038/s41467-018-03759-y

97. Lai JH, Liu YW, Lu G, *et al*. 4D bioprinting of programmed dynamic tissues. *Bioact Mater*. 2024;37:348-377.

doi: 10.1016/j.bioactmat.2024.03.033

98. Chen JY, Liang RJ, Jia SC, *et al*. Spatiotemporal Adaptation in 4D Bioprinting for Dynamic Bone and Cartilage Regeneration. *Adv Funct Mater*. 2026;36(28):e22357.

doi: 10.1002/adfm.202522357

99. Yang L, Sun Q, Chen SY, *et al*. pH-responsive hydrogel with gambogic acid and calcium nanowires for promoting mitochondrial apoptosis in osteosarcoma. *J Control Release*. 2025;377:563-577.

doi: 10.1016/j.jconrel.2024.11.055

100. Ma YC, Lai P, Sha Z, *et al*. TME-responsive nanocomposite hydrogel with targeted capacity for enhanced synergistic chemoimmunotherapy of MYC-amplified osteosarcoma. *Bioact Mater*. 2025;47:83-99.

doi: 10.1016/j.bioactmat.2025.01.006

101. Bowser DA, Moore MJ. Biofabrication of neural microphysiological systems using magnetic spheroid bioprinting. *Biofabrication*. 2020;12(1):015002.

doi: 10.1088/1758-5090/ab41b4

102. Lee G, Kim SJ, Park JK. Bioprinting of heterogeneous and multilayered cell-hydrogel constructs using continuous multi-material printing and aerosol-based crosslinking. *STAR Protoc*. 2022;3(2):101303.

doi: 10.1016/j.xpro.2022.101303

103. Pun S, Prakash A, Demaree D, *et al*. Rapid Biofabrication of an Advanced Microphysiological System Mimicking Phenotypical Heterogeneity and Drug Resistance in Glioblastoma. *Adv Healthc Mater*. 2024;13(30).

doi: 10.1002/adhm.202401876

104. Arman MS, Xu B, Tsin A, Li JZ. Laser-Induced Forward Transfer (LIFT) based Bioprinting of the Collagen I with Retina Photoreceptor Cells. *Manuf Lett*. 2023;35:477-484.

doi: 10.1016/j.mfglet.2023.07.005

105. Chang JL, Sun XM. Laser-induced forward transfer based laser bioprinting in biomedical applications. *Front Bioeng Biotechnol*. 2023;11:1255782.

doi: 10.3389/fbioe.2023.1255782

106. Duvert L, Murru C, Al-Kattan A, *et al*. Laser-induced forward transfer in picosecond regime for cell bioprinting. *Int J Bioprint*. 2025;11(2):290-301.

doi: 10.36922/ijb.7788

107. Huang WH, Chen SX, Li K, *et al*. Nanoengineered extrusion-aligned tract bioprinting enables functional repair of spinal cord injuries. *Cell Stem Cell*. 2026;33(2):340-354.e7.

doi: 10.1016/j.stem.2025.12.021

108. Wang HR, Wang C, Guo K, Zhang LM, Li S, Zheng XF. Continuous bath embedded bioprinting for high-fidelity biofriendly fabrication of complex tissues. *Mater Des*. 2026;263:115656.

doi: 10.1016/j.matdes.2026.115656

109. Grottkau BE, Hui ZX, Pang YG. Articular Cartilage Regeneration through Bioassembling Spherical Micro-Cartilage Building Blocks. *Cells*. 2022;11(20):3244.

doi: 10.3390/cells11203244

110. Jiao YG, Lu SY, Zhang JW, Zhen JP. Applications in osteochondral organoids for osteoarthritis research: from pathomimetic modeling to tissue engineering repair. *Front Bioeng Biotechnol*. 2025;13:1629608.

doi: 10.3389/fbioe.2025.1629608

111. Zuliani CC, da Cunha JB, de Souza VM, de Andrade KC, Moraes AM, Coimbra IB. Amniotic fluid MSCs for scaffold-free cartilage repair: spheroid fusion and chondrogenic microtissue development. *Future Sci OA*. 2025;11(1):2476922.

doi: 10.1080/20565623.2025.2476922

112. Varaprasad K, Karthikeyan C, Yallapu MM, Sadiku R. The significance of biomacromolecule alginate for the 3D printing of hydrogels for biomedical applications. *Int J Biol Macromol*. 2022;212:561-578.

doi: 10.1016/j.ijbiomac.2022.05.157

113. Dahlan NA, Ketabat F, Avery K, *et al*. Preparation and Characterization of Alginate-Based Bioinks for Three-Dimensional Bioprinting of Cell-Laden Constructs. *Curr Protoc*. 2025;5(12):e70290.

doi: 10.1002/cpz1.70290

114. Gonzalez-Fernandez T, Tenorio AJ, Campbell KT, Silva EA, Leach JK. Alginate-Based Bioinks for 3D Bioprinting and Fabrication of Anatomically Accurate Bone Grafts. *Tissue Eng Part A*. 2021;27(17-18):1168-1181.

doi: 10.1089/ten.tea.2020.0305

115. Kang Y, Xu J, Meng LA, *et al*. 3D bioprinting of dECM/Gel/QCS/nHAp hybrid scaffolds laden with mesenchymal stem cell-derived exosomes to improve angiogenesis and osteogenesis. *Biofabrication*. 2023;15(2):024103.

doi: 10.1088/1758-5090/acb6b8

116. Wang Q, Xia QQ, Wu Y, *et al*. 3D-Printed Atsttrin-Incorporated Alginate/Hydroxyapatite Scaffold Promotes Bone Defect Regeneration with TNF/TNFR Signaling Involvement. *Adv Healthc Mater*. 2015;4(11):1701-1708.

doi: 10.1002/adhm.201500211

117. Barrs RW, Jia J, Ward M, *et al*. Engineering a Chemically Defined Hydrogel Bioink for Direct Bioprinting of Microvasculature. *Biomacromolecules*. 2021;22(2):275-288.

doi: 10.1021/acs.biomac.0c00947

118. Lin CC, Frahm E, Afolabi FO. Orthogonally Crosslinked Gelatin-Norbornene Hydrogels for Biomedical Applications. *Macromol Biosci*. 2024;24(2).

doi: 10.1002/mabi.202300371

119. Kulikova Y, Noskova S, Barzkar N, Muravieva NA, Babich O. Review of Studies on the Application of Collagen-based Gels in Three-dimensional Printing and Bioprinting for the Production of Medical Products for Regenerative Medicine. *Biomed Biotechnol Res J*. 2025;9(4):345-352.

doi: 10.4103/bbrj.bbrj_297_25

120. Osidak EO, Karalkin PA, Osidak MS, *et al*. Viscoll collagen solution as a novel bioink for direct 3D bioprinting. *J Mater Sci Mater Med*. 2019;30(3):31.

doi: 10.1007/s10856-019-6233-y

121. Reynolds DS, de Lázaro I, Blache ML, *et al*. Microporogen-Structured Collagen Matrices for Embedded Bioprinting of Tumor Models for Immuno-Oncology. *Adv Mater*. 2023;35(33).

doi: 10.1002/adma.202210748

122. Li SL, Tian XH, Fan J, Tong H, Ao Q, Wang XH. Chitosans for Tissue Repair and Organ Three-Dimensional (3D) Bioprinting. *Micromachines*. 2019;10(11):765.

doi: 10.3390/mi10110765

123. Xu JQ, Zhang MY, Du WZ, Zhao JH, Ling GX, Zhang P. Chitosan-based high-strength supramolecular hydrogels for 3D bioprinting. *Int J Biol Macromol*. 2022;219:545-557.

doi: 10.1016/j.ijbiomac.2022.07.206

124. Butler HM, Naseri E, MacDonald DS, Tasker RA, Ahmadi A. Optimization of starch- and chitosan-based bio-inks for 3D bioprinting of scaffolds for neural cell growth. *Materialia*. 2020;12:100737.

doi: 10.1016/j.mtla.2020.100737

125. Maturavongsadit P, Narayanan LK, Chansoria P, Shirwaiker R, Benhabbour SR. Cell-Laden Nanocellulose/Chitosan-Based Bioinks for 3D Bioprinting and Enhanced Osteogenic Cell Differentiation. *ACS Appl Bio Mater*. 2021;4(3):2342-2353.

doi: 10.1021/acsabm.0c01108

126. Hidaka M, Sakai S. Photo- and Schiff Base-Crosslinkable Chitosan/Oxidized Glucomannan Composite Hydrogel for 3D Bioprinting. *Polysaccharides*. 2025;6(1):19.

doi: 10.3390/polysaccharides6010019

127. Kim S, Han S, Lee J, Lee C, Park S. Bioprinting of tumor immune microenvironment for immunotherapy. *Int J Bioprint*. 2024;10(5):31-46.

doi: 10.36922/ijb.3988

128. Mörö A, Samanta S, Honkamäki L, *et al*. Hyaluronic acid based next generation bioink for 3D bioprinting of human stem cell derived corneal stromal model with innervation. *Biofabrication*. 2022;15(1):015020.

doi: 10.1088/1758-5090/acab34

129. Weis M, Shan JW, Kuhlmann M, Jungst T, Tessmar J, Groll J. Evaluation of Hydrogels Based on Oxidized Hyaluronic Acid for Bioprinting. *Gels*. 2018;4(4):82.

doi: 10.3390/gels4040082

130. Banigo AT, Nauta L, Zoetebier B, Karperien M. Coaxial Bioprinting of Enzymatically Crosslinkable Hyaluronic Acid-Tyramine Bioinks for Tissue Regeneration. *Polymers*. 2024;16(17):2470.

doi: 10.3390/polym16172470

131. Honkamäki L, Kulta O, Puistola P, *et al*. Hyaluronic Acid-Based 3D Bioprinted Hydrogel Structure for Directed Axonal Guidance and Modeling Innervation In Vitro. *Adv Healthc Mater*. 2025;14(1):2402504.

doi: 10.1002/adhm.202402504

132. Prestwich GD. Hyaluronic acid-based clinical biomaterials derived for cell and molecule delivery in regenerative medicine. *J Control Release*. 2011;155(2):193-199.

doi: 10.1016/j.jconrel.2011.04.007

133. Poldervaart MT, Goversen B, de Ruijter M, *et al*. 3D bioprinting of methacrylated hyaluronic acid (MeHA) hydrogel with intrinsic osteogenicity. *PLoS One*. 2017;12(6):e0177628.

doi: 10.1371/journal.pone.0177628

134. Sanchez AA, Teixeira FC, Casademunt P, Beeren I, Moroni L, Mota C. Enhanced osteogenic differentiation in hyaluronic acid methacrylate (HAMA) matrix: a comparative study of hPDC and hBMSC spheroids for bone tissue engineering. *Biofabrication*. 2025;17(2):025013.

doi: 10.1088/1758-5090/adb2e6

135. Costa JB, Silva-Correia J, Oliveira JM, Reis RL. Fast Setting Silk Fibroin Bioink for Bioprinting of Patient-Specific Memory-Shape Implants. *Adv Healthc Mater*. 2017;6(22):1701021.

doi: 10.1002/adhm.201701021

136. Wu XF, Chen K, Zhang DK, Xu LM, Yang XH. Study on the technology and properties of 3D bioprinting SF/GT/n-HA composite scaffolds. *Mater Lett*. 2019;238:89-92.

doi: 10.1016/j.matlet.2018.11.151

137. Compaan AM, Christensen K, Huang Y. Inkjet Bioprinting of 3D Silk Fibroin Cellular Constructs Using Sacrificial Alginate. *ACS Biomater Sci Eng*. 2017;3(8):1519-1526.

doi: 10.1021/acsbiomaterials.6b00432

138. Liu SM, Ge CH, Li ZQ, *et al*. Visible-Light-Induced Silk Fibroin Hydrogels with Carbon Quantum Dots as Initiators for 3D Bioprinting Applications. *ACS Biomater Sci Eng*. 2024;10(9):5822-5831.

doi: 10.1021/acsbiomaterials.4c01189

139. Zhang X, Wu WB, Huang YL, Yang X, Gou ML. Antheraea pernyi silk fibroin bioinks for digital light processing 3D printing. *Int J Bioprint*. 2023;9(5):239-257.

doi: 10.18063/ijb.760

140. Domingues MF, Silva JC, Sanjuan-Alberte P. From Spheroids to Bioprinting: A Literature Review on Biomanufacturing Strategies of 3D In Vitro Osteosarcoma Models. *Adv Ther*. 2024;7(11).

doi: 10.1002/adtp.202400047

141. Khosropanah MH, Rajabi M, Tanourlouee SB, Azimzadeh A, Vaghasloo MA, Hassannejad Z. Silk as a promising biomaterial for 3D bioprinting: a comprehensive review of Bombyx mori silk's biomedical applications. *Int J Polym Mater Polym Biomater*. 2025;74(6):538-554.

doi: 10.1080/00914037.2024.2344608

142. Rajput M, Mondal P, Yadav P, Chatterjee K. Light-based 3D bioprinting of bone tissue scaffolds with tunable mechanical properties and architecture from photocurable silk fibroin. *Int J Biol Macromol*. 2022;202:644-656.

doi: 10.1016/j.ijbiomac.2022.01.081

143. Moore CA, Siddiqui Z, Carney GJ, *et al*. A 3D Bioprinted Material That Recapitulates the Perivascular Bone Marrow Structure for Sustained Hematopoietic and Cancer Models. *Polymers*. 2021;13(4):480.

doi: 10.3390/polym13040480